SPATIAL AND TEMPORAL VARIABILITY OF CHLOROPHYLL CONCENTRATIONS FROM NIMBUS - 7 COASTAL ZONE COLOUR SCANNER DATA IN THE BENGUELA UPWELLING SYSTEM AND THE SUBTROPICAL CONVERGENCE REGION SOUTH OF AFRICA

by

SCARLA JEANNE WEEKS

A Thesis submitted to the Department of Oceanography,
University of Cape Town
in fulfillment of the requirements for the
degree of Master of Science

October 1992

CONTENTS

ABSTRACT

South African oceanographers were engaged in collecting hydrographic and biological sea truth data in order to calibrate the CZCS measurements from the NIMBUS-7 satellite over the Benguela Upwelling region and along the east coast of South Africa during the period 1978 to 1981. A brief overview of the CZCS validation programme and its application to the South African marine environment is given, followed by an analysis of level-III CZCS data obtained from NASA for the region 10^{o} - 60^{o}S, and 10^{o} - 100^{o}E. This area includes the Benguela Upwelling system on the continental shelf, and the Southern Ocean with the Subtropical Convergence zone south of Africa.

High annual values (5mg m^{-3}) of chlorophyll occurred in the Benguela shelf region, typical of other upwelling systems in the world ocean, and the data shows a strong interannual signal in the seven years of composited data from 1978-1985, with maxima in 1982. Two distinct regimes were found in the Benguela Upwelling system, the seasonal variations of pigment concentration in the northern and southern Benguela regions being out of phase.

In the Southern Ocean, the values of chlorophyll were generally low (0.15mg m^{-3}) with the strongest signal (1.5mg m^{-3}) found at the southern border of the Agulhas retroflection region and its frontal boundary with the colder subantarctic water to the south. The high values of chlorophyll found in this region are ten times the typical open Southern Ocean values. There is a clear interannual signal in the CZCS data for this Subtropical Convergence region, which has a low value in 1979 rising to a maximum in 1981 and then decreasing to another low value in 1985. There appears to be no pronounced seasonal variation in the Subtropical Convergence data. Reasons for the strong signal in the surface chlorophyll concentrations at the front between the Agulhas Return Current and the Southern Ocean are discussed, and it is shown that the Agulhas Plateau sets up a topographic

Rossby wave in the Agulhas Return Current, which can be clearly identified in the CZCS signal. The large expanse of the Subtropical Convergence region is found as able to sustain a standing stock of phytoplankton similar in magnitude to that on the Benguela shelf, for limited periods of time.

A brief analysis of sea surface temperature versus chlorophyll concentration shows the relationship between the two parameters to take the form of an inverted parabola, having a temperature window within which maximum chlorophyll concentrations are found.

ACKNOWLEDEMENTS

The Foundation for Research Development Benguela Ecology Programme Phase III and the South African Antarctic Programme are gratefully acknowledged for their support of this study. Sincere appreciation is extended to Dr. F.A. Shillington of the Department of Physical Oceanography, University of Cape Town for his excellent supervision and guidance throughout the course of this study.

Special thanks are extended to Gene Feldman and his group at NASA GSFC, with particular mention of Jeff Whiting for his untiring efforts in assisting with the data acquisition, and to Chuck McClain and Gary Fu for software assistance. Ruby Lassanyi from the Jet Propulsion Laboratory PO.DAAC is also thanked for her kind assistance in acquiring MCSST data.

I would also like to thank Prof. Geoff Brundrit, Prof. John Field, Dr. Mark Jury, Shaun Courtney, Colin Attwood and Roy van Ballegooyen of the University of Cape Town, and Drs. Larry Hutchings and Penny Brown of the Sea Fisheries Research Institute for helpful discussions and assistance during the development of this thesis. Prof. Will de Ruijter is also acknowledged for his constructive comments on the Agulhas Current.

Finally, I would like to express special thanks to my husband, Andrew Hoek, for his patience, support and encouragement throughout the period of this study.

LIST OF TABLES

LIST OF FIGURES

LIST OF PLATES

CHAPTER 1

INTRODUCTION AND LITERATURE REVIEW

In the austral summer of 1978/79, South African oceanographers began a three year collaboration with the National Aeronautics and Space Administration (NASA) as part of the Nimbus-7 Coastal Zone Colour Scanner (CZCS) validation programme. The South African Ocean Colour and Upwelling Experiment emerged, the main emphasis being placed on the validation and application of the CZCS in the estimation of chlorophyll in the Benguela Upwelling region, although the east coast and southern Agulhas were also included in the programme.

The CZCS was developed by NASA, based on the principle that variability in optical properties of the open ocean is determined primarily by variability in the distribution of phytoplankton and its associated pigments: ocean colour shifts from blue to green as the concentration of phytoplankton pigments increases [*Feldman et al.*, 1989]. The Nimbus-7 spacecraft, carrying *inter-alia* the CZCS, was launched into an ascending sun-synchronous orbit in October 1978, and remained operational for seven and a half years. A comprehensive description of the CZCS and its performance is given by *Hovis et al.* [1980]. The CZCS was a multispectral scanner with a cross-track swath width of 1566km and a spatial resolution of 0.825km x 0.825km at nadir. It measured radiance at six spectral bands centred at 443, 520, 550, 670, 750nm and 11.5 μm, the first five sensing backscattered solar radiance and the sixth, emitted thermal radiance. The range of the first four spectral bands, each 20 nanometers in width, was set primarily for ocean colour and was adjustable through four sets of gains to allow for varying sun angles. Channel 5, with a 100 nanometer bandwidth, was more suited to land, while channel 6, which stopped operating after one year [*Williams, Szajna and Hovis,* 1985], was used to derive sea surface temperature (SST). The radiometer was also able to tilt

20^{o} ahead or behind the spacecraft in order to avoid sunglint from capillary waves due to the solar elevation angle.

Prior to the launch of the Nimbus-7 satellite, *Gordon and Clark* [1980] showed empirically that sea surface spectral radiance ratios are related to the sum of the photosynthetically active phytoplankton pigment, chlorophyll-*a*, and its by-product, phaeopigment-*a*, and presented algorithms for the derivation of phytoplankton pigment concentrations from CZCS radiances. Post-launch validation cruises proved these algorithms to be accurate to within a factor of two [*Gordon et al.*, 1980; *Morel,* 1980]. However, the radiances received by the CZCS sensor consisted of components due to scattering of solar irradiance from the air (Rayleigh scattering), from particles suspended in the air, from the ocean surface and from water molecules and suspended particles within the ocean. The last component is the only portion which contains any information about the concentration of phytoplankton pigments. Since the preliminary pigment algorithms were developed from measurements of surface pigment values only, *Clark* [1981] reworked these based on additional data from post-launch validation cruises, such that the depth dependence of the optical signal and the vertical distribution of phytoplankton were included. This showed only minor changes from the initial analysis even though the post-launch validation cruises sampled a large diversity of water masses, and the preliminary algorithms remained essentially unchanged. The bio-optical algorithms proposed by *Clark* [1981] are as follows:

$$C_W = A_i + B_i(\log R_i), \text{ where}$$

$$R_1 = L_{443} / L_{550},\ A_1 = -0.116,\ B_1 = -1.33$$

$$R_2 = L_{520} / L_{550},\ A_2 = +0.229,\ B_2 = -4.45,$$

C_W is the satellite-weighted chlorophyll concentration (mg m^{-3}) and L is the subsurface upwelled radiance at the specific wavelength. *Clark* [1981] showed that

any differences from the prelaunch algorithms were not due to the optical weighting - for an homogeneous ocean (Type I waters) about 90% of the backscattered irradiance originates from above the first attenuation depth, defined as $Z_{90} = {}^{1}/_{K(\lambda)}$, where $K(\lambda)$ is the diffuse attenuation coefficient in water for light at that wavelength [*Gordon and McCluney*, 1975] - but due to sampling in turbid waters (Type II waters). Since differences occurred especially for upwelled radiances at 443nm, R_1 should only be used for chlorophyll concentrations less than 1.5mg m^{-3}. *Clark* [1981] suggested that the distribution of chlorophyll is not highly variable above the first attenuation depth in Type I waters (approximately 10 - 20m) and that the above bio-optical algorithms may be used globally to provide estimates of chlorophyll concentrations accurate to within 35% in Type I waters, and within a factor of 2 in all waters. These factors were confirmed by *Gordon and Morel* [1983].

As part of the CZCS validation programme, a series of ocean colour experiments were undertaken in the southern Benguela region and along the east coast of southern Africa. The main objectives of the South African surface-truth ocean-colour experiments were to relate the CZCS radiance measurements to chlorophyll distributions, organic pollution, upwelling fronts, suspended sediments, and to thermal fronts in the southern Agulhas region. The major achievements of the South African Ocean Colour Experiment have been published in a volume of eighteen papers edited by *Shannon* [1985a]. Amongst others, extensive physical, biological and meteorological measurements were made to develop algorithms suitable for the South African marine environment. *Walters, Kok and Claase* [1985] describe the results of the optical shipboard measurements and their application locally. *Walters* [1985] determined suitable bio-optical algorithms to relate ratios of upwelled radiances to chlorophyll concentrations for South African waters, the chlorophyll concentrations being optically weighted over one attenuation depth. He suggested, however, that the L_{443}/L_{550} ratio only be used for

concentrations of less than 0.6mg m^{-3}. Similar to *Clark* [1981], *Walters, Kok and Claase* [1985] showed that the optical weighting did not significantly change the surface chlorophyll values in Type I waters, and concluded that the bio-optical algorithms presented by *Clark* [1981] can be used to determine chlorophyll concentrations along the Cape west coast, but were not suited to the east coast waters which contain high concentrations of terrigenous materials. These bio-optical algorithms were subsequently used in the successful analysis of West Coast CZCS data [*Walters, 1983; Shannon, Schlittenhardt and Mostert, 1984; Shannon, Walters and Mostert, 1985*], and in the southern Agulhas region [*Lutjeharms and Walters,* 1985], also characterized as type I water. The algorithms were further modified in order to semi-quantify the distribution of suspended sediments along the Cape east coast, where Type II waters are found [*Walters and Schumann,* 1985].

During its seven and a half year lifetime, the CZCS acquired around 66 000 two minute scenes. The NASA Goddard Space Flight Centre (GSFC) together with the University of Miami/Rosenstiel School of Marine and Atmospheric Science, undertook to process the entire CZCS data set and to make the data products accessible to the international oceanographic community [*Esaias et al.*, 1986]. The entire level-I data set has now been processed to levels-II and -III and represent the most comprehensive source of ocean colour measurements to date [*Feldman et al.*, 1989]. A description of the level-I to -III CZCS products is given in Table 1.

Since a gradual loss of sensor sensitivity was recognized relatively early in the CZCS lifetime, especially in band 1 (443nm) [*Austin*, 1982], the generation of derived geophysical parameters from the level-Ia data (Table 1) includes decay factors necessary to correct for the sensor degradation [*Feldman et al.*, 1989]. The processing procedures also incorporate ozone concentrations derived from the Total Ozone Mapping Spectrometer to correct for Chappieu band absorbance errors and eliminate data severely effected by cloud ringing and sunglint [*Feldman et al.*,

1989]. It is also necessary to mention that the atmosphere contributed 80 to 90% of the total radiance received by the CZCS and that this needs to be corrected for before accurate estimates of the water-leaving radiance, from which chlorophyll concentration is computed, can be made. In the generation of the data products listed in Table 1, a multiple Rayleigh scattering model with full polarization effects was used and a standard atmospheric aerosol type was assumed: the Angstrom exponents were taken as zero. *Feldman et al.* [1989] states that this aerosol correction is valid for most open ocean regions. Also, the *Clark* [1981] algorithms were used to estimate pigment concentrations from water-leaving radiances, since several regional studies had shown the validity of this relationship [*Feldman et al.*, 1989], achieving accuracies to within 35% in Type I waters and within a factor of two generally [*Walters, Kok and Claase*, 1985; *Esaias et al*, 1986; *Feldman*, 1986].

TABLE 1. THE CZCS DATA PRODUCTS.

LEVEL	DESCRIPTION	SPATIAL RESOLUTION
Level-I	Calibrated radiances for all six CZCS channels, and earth location information for a single CZCS scene (maximum 2 min of data) in std. CRIT format.	1km
Level-Ia	Subsampled Level-I data: every 4th pixel, every 4th line, in DSP (University of Miami) format for bands 1-5.	4km
Level-II	Derived geophysical parameters for a single CZCS scene in DSP format. The 6 derived products are: Phytoplankton pigment concentration, Diffuse attenuation coefficient, Normalized water-leaving radiance at 440nm (nlw440), nlw520, nlw 550, and Aerosol radiance at 670nm.	4km
Level-III	Composited earth-gridded data of the Level-II parameters binned to a fixed latitude-longitude array of dimension 1024 by 2048.	18.5km at the equator

Adapted from Feldman et al [1989]

An important aspect of the CZCS scanner is that operation was limited to about 10% of its cycle [*Feldman et al.*, 1989], or a maximum of two hours per day, due to spacecraft power constraints. Coverage was not uniformly distributed around the globe, 70% of radiance measurements being obtained from the Northern Hemisphere [*McClain et al.*, 1991]. As a result, the number of daily valid chlorophyll measurements that make up a monthly level-III composite (Table 1) often shows the sampling to have been highly skewed. This can introduce errors when considering a level-III composite as representative of a long-term mean. However, although individual scenes represent the best temporal resolution for resolving individual features, it is only by compositing over longer time scales that a better understanding of the distribution and variability of phytoplankton pigment concentration on the synoptic and global scale may be obtained.

Over the last decade, application of CZCS data has progressed from scene by scene studies to regional time series, with ocean-basin and global-scale analysis only recently begun: *McClain et al.* [1990] examined the seasonal cycle of the phytoplankton biomass in the North Atlantic Ocean using monthly CZCS pigment composites. They showed that the shelf and open ocean regions have spring and fall phytoplankton blooms of equal magnitude and illustrated the relationship between phytoplankton biomass and local physical forcing. *Muller-Karger et al.* [1991] derived monthly CZCS and SST composites for the Gulf of Mexico, showing that, seaward of the shelf, the seasonal variations in pigment concentration and sea surface temperature are synchronous throughout the Gulf, although out of phase relative to one another. In contrast, they found the phases of pigment concentration and mixed layer depth to be similar, and suggested that the most important factor controlling the seasonal variation in pigment concentration is the depth of the mixed layer. *Morel and Andre* [1991] analysed a set of 114 CZCS images to describe the evolution of algal biomass in the western Mediterranean and, using a spectral light-photosynthesis model, estimated the potential carbon fixation.

They found a six-fold seasonal variation in primary production within the northern zone, with only a two-fold variation in the southern zone. *Brock and McClain* [1992] used CZCS imagery for the period 1979 through 1982 together with *in situ* hydrographic and meteorological data to relate the interannual variations in the northern summer phytoplankton blooms to changes in surface-level southwest monsoon winds. The phytoplankton blooms in the northwestern Arabian Sea were shown to peak during August-September, lagging the open ocean upwelling by about one month, and reached maximum values during the late phase of 1980 when the southwesterlies were strongest. *Sousa and Bricaud* [1992] examined the spatial and temporal distribution of phytoplankton pigment in Portuguese coastal waters using CZCS images for the period July 1981 to September 1983. No significant spatial patterns were found during the northern winter and spring, while several recurrent patterns were observed during the upwelling season from June to October. A significant relationship was found between the temporal variability of these patterns and the strength of the offshore Ekman transport, and a linear relationship was shown between sea surface temperature and chlorophyll concentration.

Although a large number of individual CZCS scenes in South African waters had been analysed by 1985, [*Shannon, Schlittenhardt and Mostert, 1984; Shannon, Walters and Mostert*, 1985; *Walters and Schumann,* 1985; *Lutjeharms and Walters*, 1985] a huge backlog of data processing halted the continued exploration of the CZCS data. With the recent level-III archive of CZCS data at NASA becoming available to oceanographers worldwide, and as a preparation for the new Sea-Viewing Wide Field-of-view Sensor (SeaWiFS) project, the author decided to examine the historical CZCS archive for the oceans around and to the south of southern Africa to determine the spatial and temporal variability of chlorophyll-*a*, and hence phytoplankton biomass near the ocean surface. The relationship between sea surface temperature and chlorophyll concentration was also briefly examined, the sea surface temperature data being measured by the Advanced Very High

Resolution Radiometer (AVHRR) on board the TIROS-N/NOAA series of polar-orbiting satellites. The primary objective of the 4 (NOAA 6, 8 and 10) or 5 channel AVHRR sensor, is to provide sea surface temperatures through passively measured visible, near infra-red and infra-red spectral radiation bands. The AVHRR sensor has an instantaneous field of view that corresponds to a ground resolution of about 1.1km at nadir, and a total scan width of about 2240km. The five spectral bands are: channel 1, visible, 0.58 to 0.68 microns; channel 2, near infrared, 0.725 to 1.10 microns; channel 3, infrared, 3.55 to 3.99 microns; channel 4, thermal infrared, 10.2 to 11.5 microns and channel 5, a second thermal infrared channel at 11.5 to 12.5 microns [*Smith*, 1992].

As an introduction to the complex flow around the southern African area, Plate 1 portrays a level-II CZCS composite of 31 March and 2 April 1984, with a 4km resolution. The very low chlorophyll concentrations (0.1mg m^{-3}) delineate the path of the Agulhas Current south of the continent and the Agulhas Bank, and also show the budding off of an Agulhas ring centred at 36^{o}S; 17^{o}E. Also evident in Plate 1 is a second Agulhas ring centred due west of Cape Town at 33^{o}S; 14^{o}E. It is clear that these two strong, dynamic structures are interacting with the chlorophyll-rich shelf waters and that shelf water was being entrained offshore at the boundaries of the two anticyclonic (anticlockwise) Agulhas rings. *Walker* [1986] examined the NOAA-7 sea surface temperature image for the same time as Plate 1 (1 April 1984), describing these anticyclonic Agulhas rings as moving northwards to intensify the Benguela upwelling fronts. Further north (29^{o}S), there is evidence of a chlorophyll-rich filament moving offshore a distance of 270 nautical miles (500km) from the coast, with a second filament of similar length located at 26^{o}N. Previous ship and satellite observations [*Lutjeharms, Shillington and Duncombe Rae, 1991; Duncombe Rae, Shillington, Agenbag et al.*, 1992] have shown that it is possible for passing Agulhas rings to form extremely long cold water filaments offshore from the Benguela Upwelling system. This filament ring interaction has been shown to

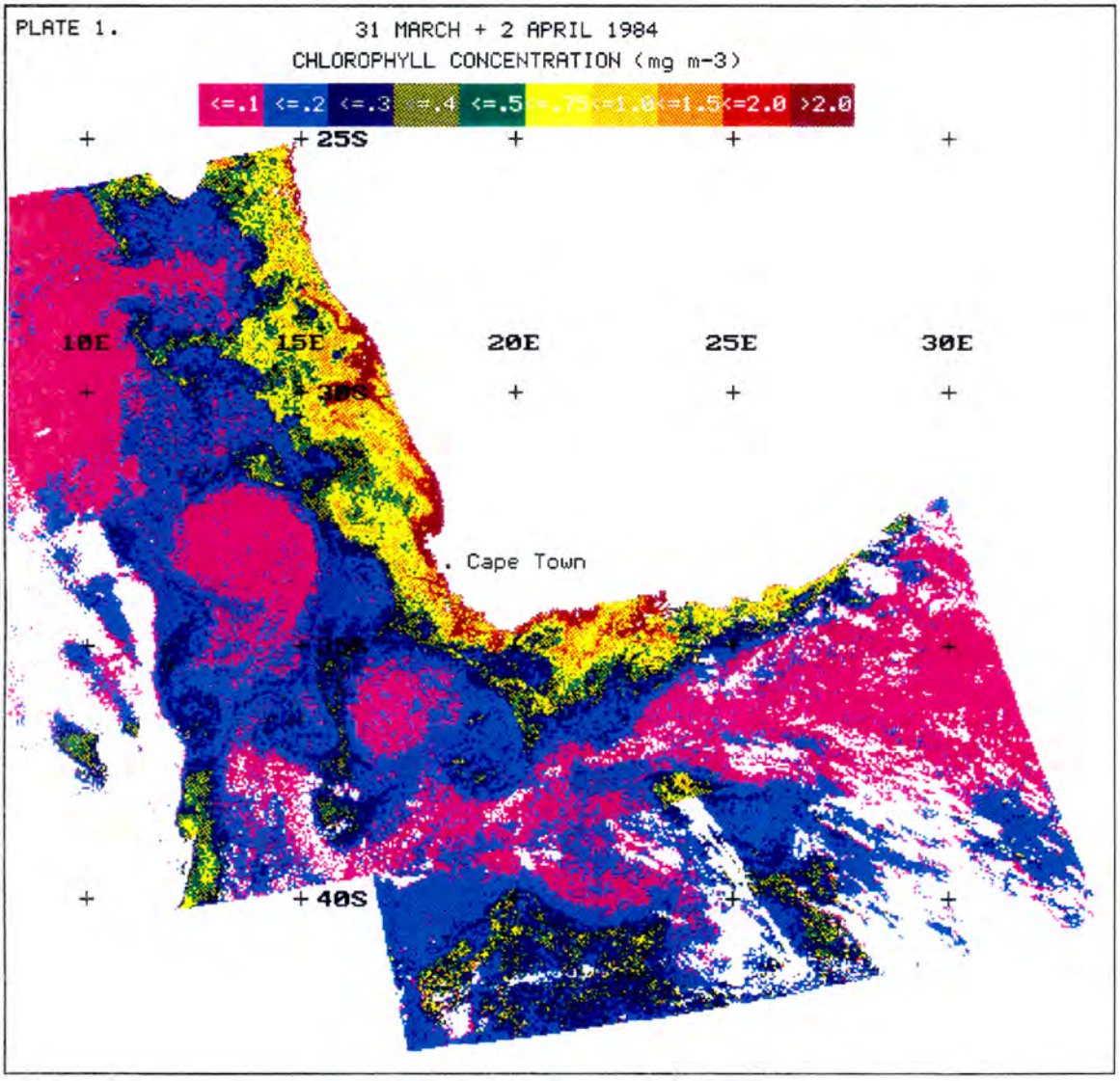

Plate 1. A CZCS composite for 31 March and 2 April 1984, with a 4km resolution, portraying the complex flow around south-western Africa. Low chlorophyll concentrations show the path of the Agulhas Current and associated Agulhas rings entraining chlorophyll-rich shelf waters. Further north, two chlorophyll-rich filaments are seen moving offshore.

persist for periods of greater than a month enabling a relatively large volume of water from the Benguela Upwelling region to encircle the ring [*Lutjeharms, Shillington and Duncombe Rae*, 1991]. South of the continent, there is evidence of high chlorophyll concentrations on the Agulhas Bank (Plate 1). However, caution should be exercised in the interpretation of the CZCS signal on the Agulhas Bank since these waters are classified as Type II waters, a deep subsurface chlorophyll maximum usually found between 20 - 60m depth [*Peterson et al.*, 1992]. Further more detailed reviews on the Benguela Ecosystem, its physical and biological processes are given by *Shannon* [1985b] and *Shannon and Pillar* [1986], while an overview of the Agulhas retroflection rings in the South Atlantic Ocean is given by *Duncombe Rae* [1991].

CHAPTER 2

DATA SETS AND DATA ANALYSIS

The full seven and a half year CZCS level-III data set for the Indian Ocean region, generated by the NASA GSFC processing team [*Feldman et al.*, 1989], was used for this study. These regional level-III products are 512 x 512 subarrays of the original standard global gridded data with dimensions of 1024 (north - south) x 2048 (east - west) pixels. The Indian Ocean 512 x 512 pixel subarray corresponds to the area 31.03^{o}N to 58.80^{o}S, and 10.81^{o}E to 100.64^{o}E, with a resolution of about 19.5km at the equator. The dataset includes the mean monthly and 3-monthly composites, each representing all the validated CZCS images within the Indian Ocean region for that period, binned together to form a mean pigment composite. Thus, for the Southern Hemisphere, all the validated CZCS images for the quarterly periods January to March, April to June, July to September, and October to December, represent summer, fall, winter and spring, respectively. In addition, a video generated from the CZCS browse program [*Feldman et al.*, 1989] was used to select specific level-II images, in order to resolve individual features characteristic within the area of interest, such as that seen above in Plate 1.

The datasets were ingested and analysed using the PC-SEAPAK software package developed at NASA GSFC [*Firestone et al.*, 1990; *McClain et al.*, 1992; *Darzi et al.*, 1991], the data representing phytoplankton pigment according to the log scale 'pigment = 10^(pixel value * 0.012 - 1.4)'. The U.S. Navy digital bathymetry dataset, which contains depth data at a resolution of 5 x 5 minutes for the world oceans, was used to generate a bathymetric image for the Indian Ocean region. All level-III images were mapped to a cylindrical equirectangular projection. Since the level-III Indian Ocean region covers a somewhat larger area than was of interest to this study, the area was further subsampled to include only that area south of latitude 12^{o}S. This region (12^{o}S to 60^{o}S, and 10^{o}E to 100^{o}E) includes the

Benguela Upwelling system on the continental shelf of south-west Africa (Plate 1), and the Subtropical Convergence front in the Southern Ocean. The Subtropical Convergence is classically thought of as a region in which denser subantarctic surface water subducts northwards beneath the subtropical surface water to form the South Atlantic and Indian Ocean central water [*Sverdrup, Johnson and Fleming*, 1942]. South of Africa, the Subtropical Convergence exhibits the strongest horizontal thermal and saline gradients, both at the surface and at depth [*Lutjeharms and Valentine*, 1984], and has been shown to be an area in which enhanced concentrations of chlorophyll and phytoplankton standing stock are to be found [*Planke*, 1977; *Allanson, Hart and Lutjeharms*, 1981].

The annual level-III composites as provided by NASA GSFC, extend from January to December for each year, thus not suitably representing the austral climatological year. Austral annual composites were therefore created by compositing the mean monthly images from October to September of the following year to form 7 annual composites extending from Spring 1978 to Winter 1985. Similarly, the mean seasonal images for the full seven and a half year dataset were composited by season, to form austral seasonal composites. Thus, for example, Plate 2 represents the mean pigment concentrations for all the austral summers from 1979 to 1986.

An initial analysis of the level-III data revealed the relative paucity of the data density - only about 30% of the global CZCS data was obtained from the Southern Hemisphere [*McClain et al*, 1991]. It soon became apparent that the mean 3-monthly (seasonal) composite was the minimum period that should be considered to assess the temporal variability within this area. Further analysis of these mean seasonal pigment composites showed sampling to be markedly skewed towards the west, such that the data density east of about 50^{o}E was extremely sparse, particularly in the higher latitudes. Since two marked chlorophyll signals were clearly evident in the area of interest (Plate 2), namely the Benguela Upwelling

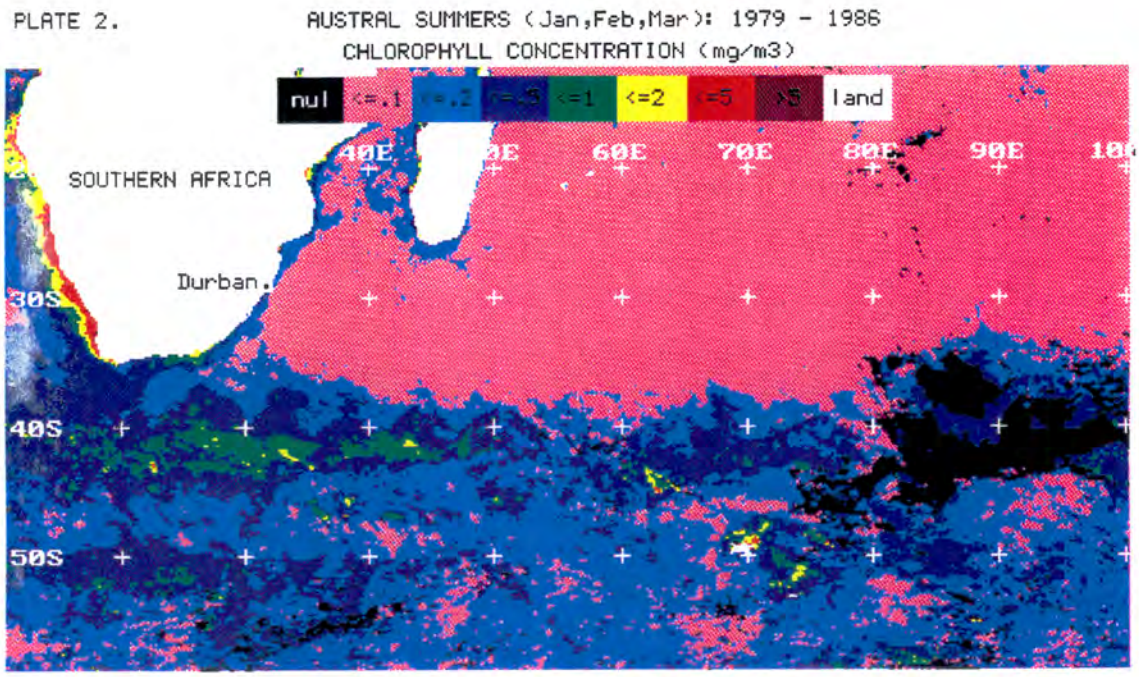

Plate 2. CZCS composite representing the mean pigment concentrations for all the austral summers from 1979 to 1986. Two marked chlorophyll signals are evident, namely the Benguela Upwelling system on the southwest African continental shelf, and, in the Southern Ocean, the Subtropical Convergence front around 41°S.

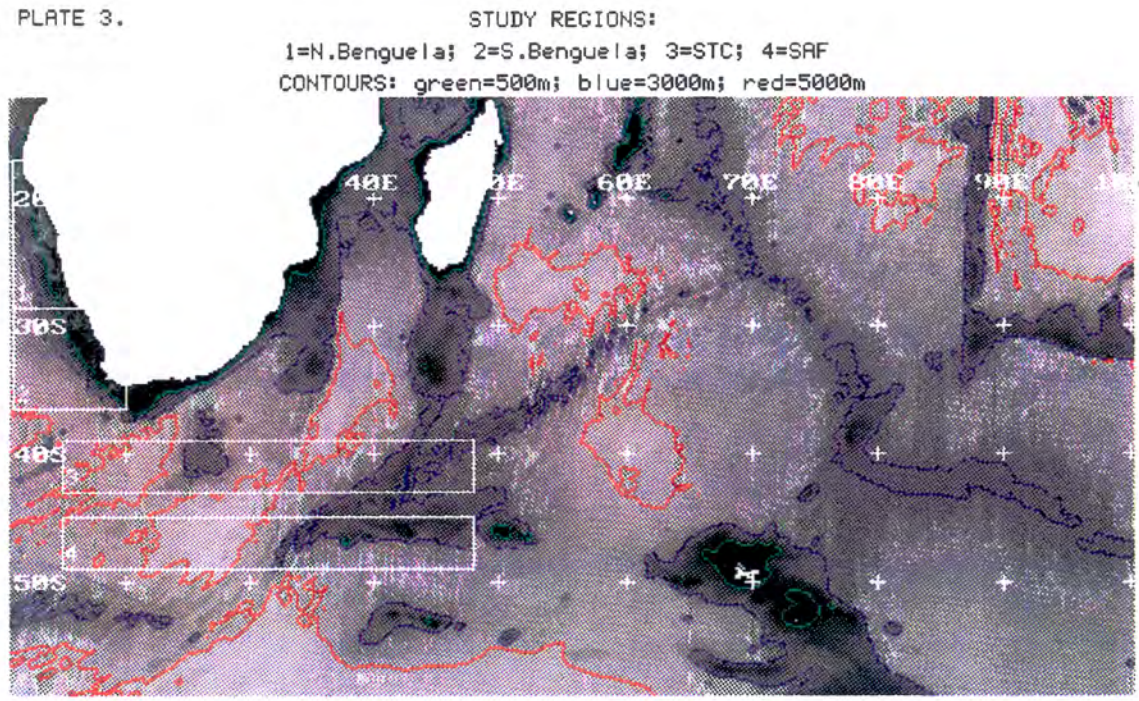

Plate 3. A bathymetric image for the area of interest showing the regions delineated for detailed analysis: the northern and southern Benguela regions extending out to the 500m isobath, and the Subtropical Convergence and Subantarctic frontal regions to the south of Africa.

system on the southwest African continental shelf, and the Subtropical Convergence zone around latitude 41°S, it was decided to concentrate on the relative contributions to oceanic biological productivity of these two contrasting areas, a shelf and an open ocean frontal region. Hence, four specific areas within the more frequently sampled regions, were delineated for further detailed analysis, as shown in Plate 3. Using the generated bathymetric image, the 500m depth contour was selected to discriminate between the continental shelf and open ocean, the shelf in this region being both narrow and very steep beyond the 500m isobath.

The Benguela region was thus demarcated as extending from the Cunene River (17°S) in the north to the intercept of the 500m isobath with the 20°E longitude in the south (Plate 3), being separated into northern and southern Benguela regions at the latitude of the Orange River (28.5°S). These areas were later subdivided into inner shelf and outer shelf substrata by the 200m isobath for detailed seasonal analysis. The two frontal areas south of Africa selected for further study (Plate 3) were the Subtropical Convergence region exhibiting a marked chlorophyll signal (Plate 2) and, for comparative purposes, the Subantarctic Front to the south. The Subtropical Convergence region was delineated to include the area 39°S to 43°S, and the Subantarctic Front 45°S to 49°S. In both cases, the area extended from 15°E to 48°E, the data to the east of this being regarded as too sparse for meaningful analysis. The limits and area of each of these regions are listed in Table 2. Because of the cylindrical equirectangular projection of the composite images, a cosine (latitude) weighting was applied to each point to transform the data to equal increments of area.

Since the full statistical count dataset, detailing the number of valid CZCS data samples within each fixed bin of a composite image, was not available, a random analysis of the available compositing statistics (1983 to 1986) was undertaken. This showed the CZCS coverage within the selected regions as being fairly constant during this period, lending confidence to the specific site selection. A later

comparative time series analysis, as detailed in Chapter 3, between the Subtropical Convergence zone and distant monsoon region of the northwestern Arabian Sea [*Brock and McClain*, 1992], reinforced our site selection since both regions are subject to Indian Ocean easterly wind stress.

TABLE 2. AREAS SPECIFIED FOR DETAILED ANALYSIS.
(ref. Plate 3)

AREA TITLE	LIMITS	AREA (km^{2}*1000)
NORTHERN BENGUELA	17°S - 28.5°S :	
	0 - 500m depth	136
Inner shelf	0 - 200m depth	53
Outer shelf	200 - 500m depth	83
SOUTHERN BENGUELA	28.5°S - intercept :	
	500m isobath with 20°E	121
Inner shelf	0 - 200m depth	54
Outer shelf	200 - 500m depth	67
SUBTROPICAL CONVERGENCE	39°S - 43°S; 15°E - 48°E	1264
SUBANTARCTIC FRONT	45°S - 49°S; 15°E - 48°E	1143

In order to obtain some understanding of the relationship between sea surface temperature and pigment concentration, a year's sea surface temperature data was examined. The austral year October 1981 to September 1982 was selected as being the midpoint of the seven year austral annual CZCS dataset. Multi-channel sea surface temperature (MCSST) data derived from the TIROS-N/NOAA series AVHRR for the selected period were obtained from the Physical Oceanography Distributed Active Archive Centre (PO.DAAC) at the Jet Propulsion Laboratory (JPL) [*Smith*, 1992]. The MCSST product consists of a weekly composite for the

globe at approximately 18km resolution. The MCSST values are binned into a global 1024 (north - south) x 2048 (east - west) pixel grid, each grid point representing the average of all daytime MCSST measurements available for that week. Missing data are flagged and interpolated using an iterative Laplacian relaxation technique. The weekly MCSST data for the 1981 to 1982 period were ingested and transformed to SEAPAK format, such that the data represents sea surface temperature according to the linear scale 'SST (^{o}C) = pixel value * 0.125 + 0.00'. Regional 512 x 512 subarrays were extracted so as to include the area of interest, and all flagged (interpolated) data removed for the purpose of this study. The 52 weekly regional fields were processed and binned to form mean 3-monthly composites corresponding to the mean seasonal chlorophyll composites for the same period. These were then also mapped to a cylindrical equirectangular projection such that each pixel represents an area of 0.18^{o} x 0.18^{o}.

CHAPTER 3

RESULTS

3.1. SPATIAL VARIABILITY

The typical spatial distribution of chlorophyll-a in the oceans around and south of southern Africa, is clearly shown in Plate 2. Chlorophyll values in the open ocean are generally low (0.15mg m^{-3}). The warm nutrient-poor waters of the Agulhas Current are seen to closely follow the continental shelf of the south-east coast, downstream of Durban. On reaching the southern tip of the Agulhas Bank, the current continues in a southerly direction, retroflecting eastwards to form a topographic Rossby wave known as the Agulhas Return Current. Two distinct chlorophyll signals are noted: high (5mg m^{-3}) mean pigment concentrations are found in the Benguela Upwelling region confined to the continental shelf, typical of upwelling systems in the world ocean. In the Southern Ocean, the strongest signal (1.5mg m^{-3}) is found in the Subtropical Convergence zone, which forms the frontal boundary between the southern border of the Agulhas Return Current and the colder subtropical waters to the south. The high values seen in this region are almost an order of magnitude greater than typical Southern Ocean pigment values.

3.2. TEMPORAL VARIABILITY

In order to assess the temporal variability of the selected regions listed in Table 2, time series of mean pigment concentration were computed for each area. Tables 3, 5 and 6 provide the data for the seasonal, interannual and intra-annual time series, including the number of values, the mean and the standard deviation. A minimum number of "valid" values (0.04 - 34mg m^{-3}) required to compute the mean within each region is also listed for each of these areas. These values represent the number of level-III bins within that region and period and not the number of CZCS samples. For the equirectangular projection used in this study, each level-III bin or pixel represents a 0.18^{o} x 0.18^{o} area and comprises the mean of all CZCS samples that fall within that bin's area for that period. In this study, the number of CZCS samples used to compute the mean pigment value for each level-III bin was not used to weight the bin's contribution to the region's mean and standard deviation. In cases where the minimum number of "valid" values was not met, as occurred in the intra-annual time series, the data point was replaced by an interpolated mean, weighted by the seasonal mean. Caution should therefore be applied when interpreting the results of this time series (Table 6) for the periods of winter 1984 to winter 1985 and summer 1984 to fall 1985, for the northern Benguela and Subantarctic Front regions, respectively.

3.2.1. Seasonal Variability

The mean seasonal variations within the Benguela and frontal regions are shown in Plate 4 and in the seasonal time series (Table 3 and Figure 1). The northern Benguela chlorophyll signal (Figure 1a) exhibits a minor peak in the spring, decreasing marginally during the summer months before rising to a maximum in the fall. This variation follows the same trend in the inner shelf and outer shelf substrata, but is most pronounced in the inner shelf substratum, where the mean chlorophyll concentration (2.7mg m^{-3}) is around one and a half times that of the

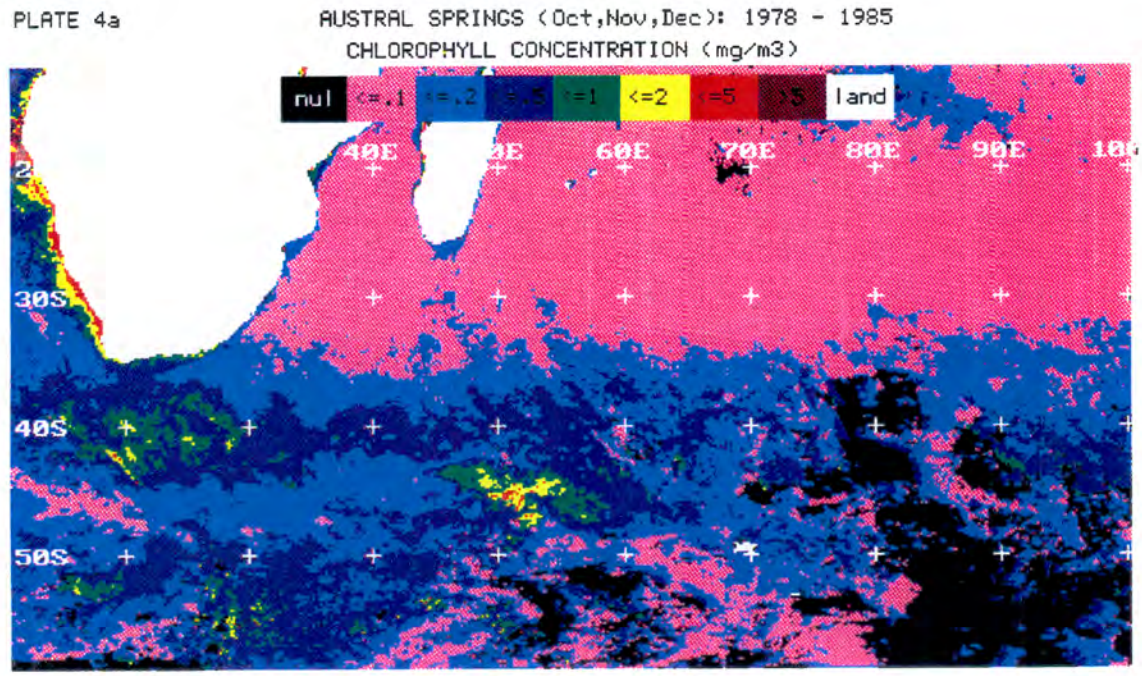

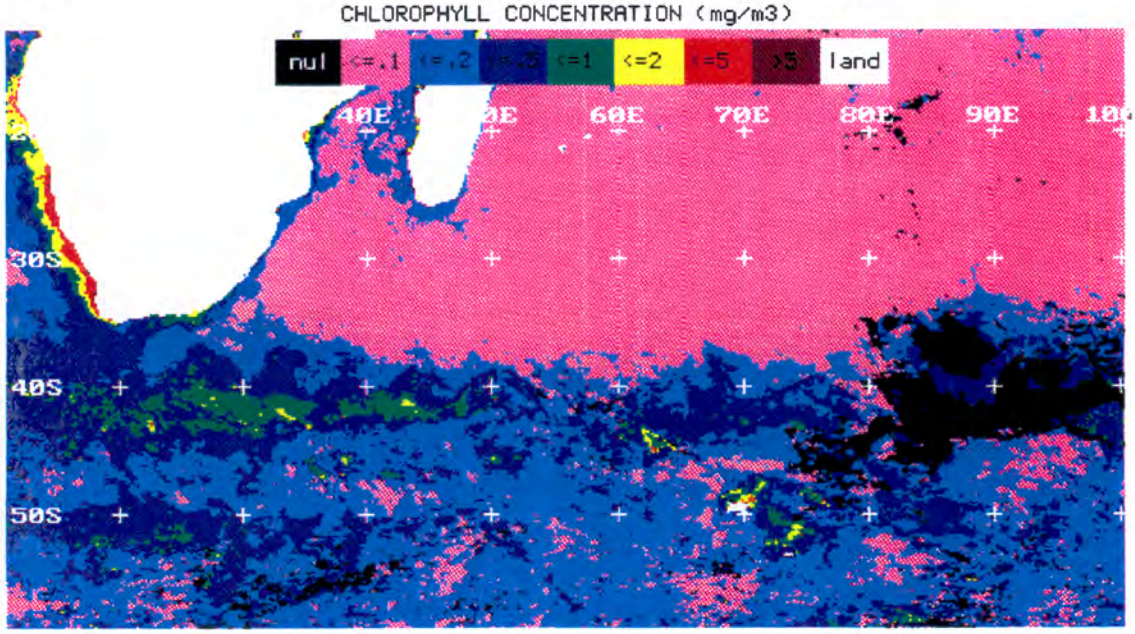

Plate 4. CZCS seasonal mean pigment concentrations for the austral seasons a) spring 1978 to 1985 and b) summer 1979 to 1986.

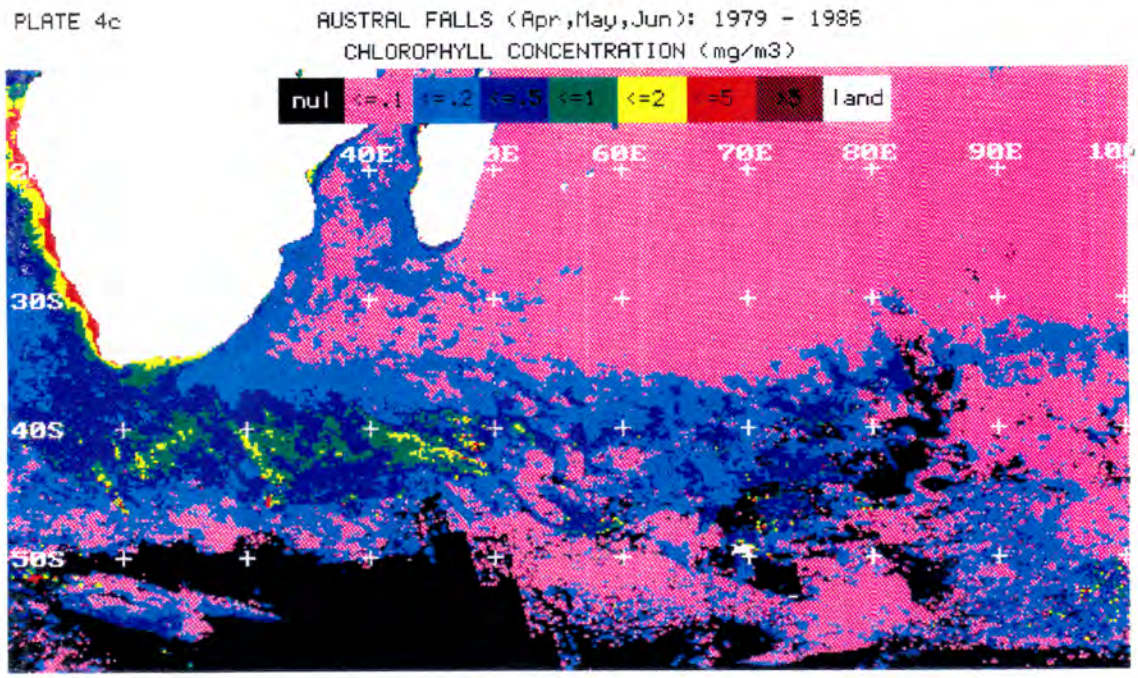

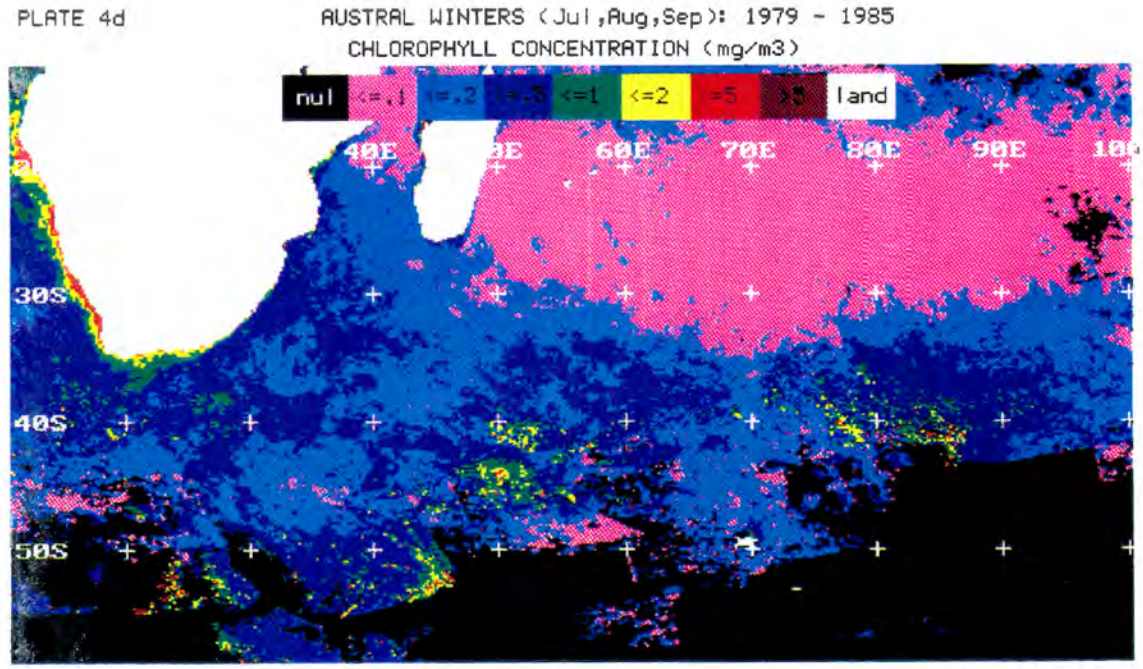

Plate 4 (continued). CZCS seasonal mean pigment concentrations for the austral seasons c) fall 1979 to 1986 and d) winter 1979 to 1985.

outer shelf substratum (1.8mg m^{-3}) (Table 3). In contrast, the southern Benguela seasonal time series shows a single chlorophyll maximum occurring during the summer months, this variation again being consistent in both the outer shelf and inner shelf substrata (Figure 1b). The maximum is not as pronounced as that occurring in the northern Benguela during the fall. However, the mean pigment concentration in the inner shelf substratum (2.3mg m^{-3}) is about twice that of the outer shelf substratum (1.1mg m^{-3}) during all 4 seasons (Table 3). The mean pigment concentration in the northern Benguela (2.1mg m^{-3}) is also, on average, 1.4 times that of the mean southern Benguela value (1.5mg m^{-3}).

TABLE 3: SEASONAL VARIATIONS (ref Figure 1).
Seasonal Means: Spring 1978 – Fall 1986

CONTINENTAL SHELF REGIONS

NORTHERN BENGUELA

	0 – 500m depth			0 – 200m depth			200 – 500m depth		
	Valid	Mean	s.d.	Valid	Mean	s.d.	Valid	Mean	s.d.
SPRING	386	2.08	1.99	151	2.71	1.86	292	1.90	2.00
SUMMER	386	2.03	1.10	151	2.57	1.21	292	1.81	0.93
FALL	386	2.50	1.13	151	3.35	1.08	292	2.13	0.86
WINTER	386	1.64	0.98	151	2.25	1.05	292	1.39	0.74

SOUTHERN BENGUELA

	0 – 500m depth			0 – 200m depth			200 – 500m depth		
	Valid	Mean	s.d.	Valid	Mean	s.d.	Valid	Mean	s.d.
SPRING	368	1.26	0.95	165	1.87	1.08	261	0.91	0.56
SUMMER	368	1.87	1.29	165	2.70	1.47	261	1.48	0.97
FALL	368	1.55	1.13	165	2.32	1.24	261	1.14	0.75
WINTER	368	1.40	1.25	165	2.22	1.41	261	0.94	0.69

SOUTHERN OCEAN FRONTAL REGIONS

	SUBTROPICAL CONVERGENCE			SUBANTARCTIC FRONT		
	Valid	Mean	s.d.	Valid	Mean	s.d.
SPRING	4392	0.35	0.21	4392	0.17	0.05
SUMMER	4392	0.42	0.20	4390	0.18	0.12
FALL	4388	0.49	0.29	3945	0.17	0.32
WINTER	4383	0.24	0.11	3645	0.21	0.14

NOTE: "Valid" is the minimum number of level-III bins having values between 0.04 and 34mg/m^3. This minimum number is 100 for the northern and southern Benguela regions, 50 for the inner and outer shelf substrata, and 550 for the frontal regions.

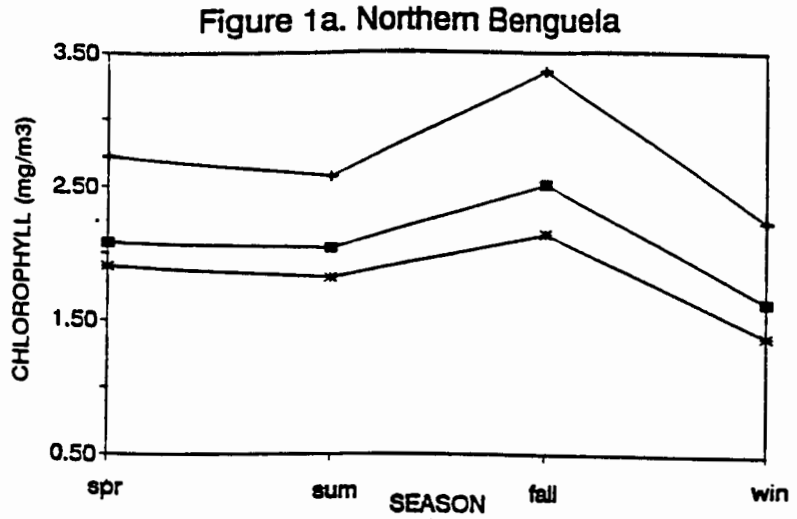

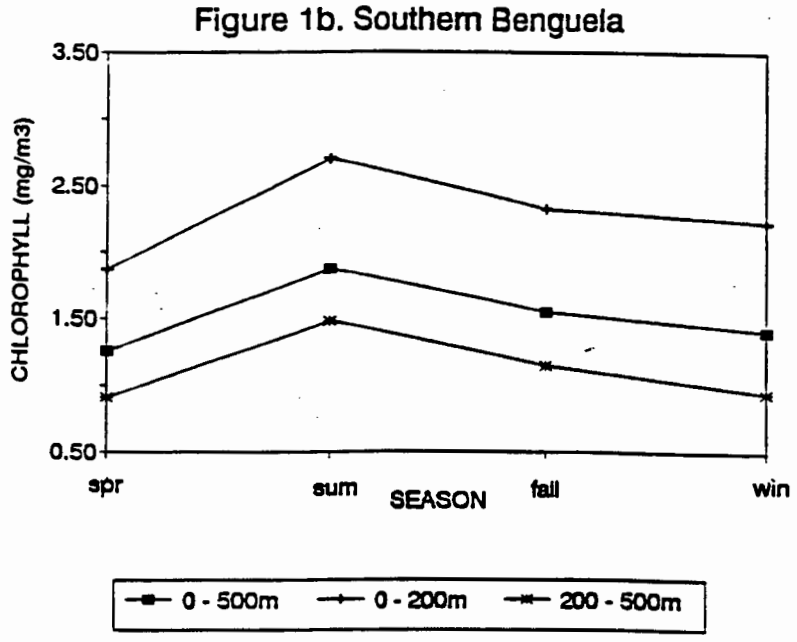

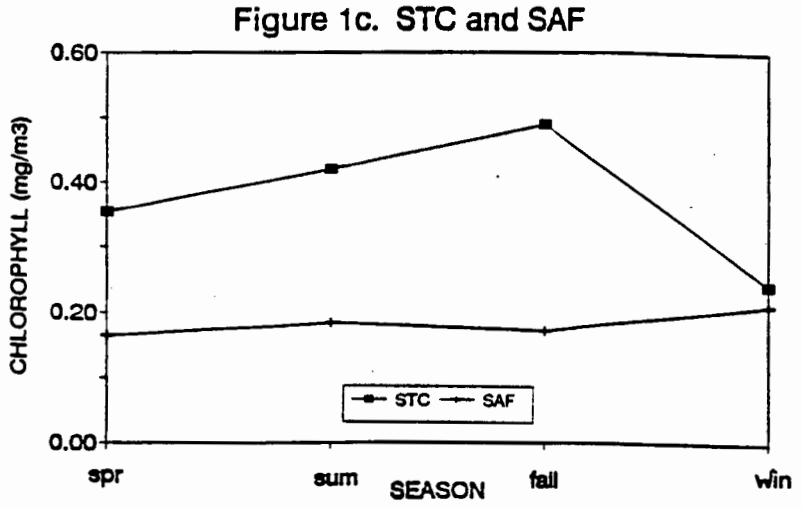

Figure 1. The seasonal time series of mean pigment concentration for the Benguela and frontal regions listed in Table 2. The northern Benguela (Figure 1a) has a minor peak in spring with a maximum in fall, while the southern Benguela (Figure 1b) has a single maximum in summer. The inner and outer shelf substrata follow the same trend in both regions, being most pronounced in the inner shelf substrata. The seasonal variation in the frontal regions (Figure 1c) is less pronounced, although the chlorophyll signal in the Subtropical Convergence region shows a maximum in fall.

The "productive area" of the shelf is defined as that area with a mean pigment concentration of greater that 2mg m^{-3}. The seasonal variations in the magnitude of the productive area are shown in Table 4 and in Figure 2. We find that, in both the northern and southern Benguela regions, the seasonal variations of the productive area (Figure 2) and mean pigment concentration (Figures 1a and 1b) are synchronous. The extent of the productive area of the Benguela (north and south) ranges from a minimum of 28% (winter) to a maximum of 50% (fall) of its total area (Table 4), while the productive area as a percentage of total area of the

TABLE 4: SEASONAL VARIATIONS OF THE BENGUELA PRODUCTIVE AREAS (ref. Figure 2). Seasonal Means: Spring 1978 – Fall 1986.

	BENGUELA REGION (northern + southern)				
	Valid	Mean	s.d.	Area (km^2) * 1000	Prod. Area as % of Whole Area (*)
SPRING	263	3.71	2.25	91	35.41
SUMMER	300	3.20	0.95	104	40.34
FALL	368	3.10	0.91	127	49.55
WINTER	209	3.05	0.92	72	28.14
	NORTHERN BENGUELA				
	Valid	Mean	s.d.	Area (km^2) * 1000	Prod. Area as % of Whole Area (*)
SPRING	186	4.07	2.55	65	48.11
SUMMER	155	3.13	0.93	54	40.09
FALL	251	3.12	0.91	88	64.93
WINTER	130	2.78	0.77	46	33.63
	SOUTHERN BENGUELA				
	Valid	Mean	s.d.	Area (km^2) * 1000	Prod. Area as % of Whole Area (*)
SPRING	73	2.87	0.70	24	19.80
SUMMER	142	3.27	0.98	46	38.52
FALL	110	3.02	0.98	36	29.84
WINTER	86	3.27	1.03	28	23.33

* : ref. Table 2

NOTE: "Valid" is the minimum number of level-III bins having values between 0.04 and 34mg/m^3. This minimum number is 200 for the whole Benguela region, and 100 for the northern and southern Benguela regions, respectively.

northern and southern Benguela respectively, range from 34% (winter) to 65% (fall) and 20% (spring) to 39% (summer). Similar results from shipboard analyses were found by *Brown and Cochrane* [1991], who also found a doubling of production area from 18% (winter) to 37% (summer) in the southern Benguela region. Their study did not include the northern Benguela region. It is worth noting that, in the northern Benguela, while the productive area is greatest in the fall, the maximum mean pigment concentration in that area occurs in spring (along with a very large standard deviation), whereas, in the southern Benguela, the mean productive area pigment value in the winter is the same as that occurring in the summer, even though the productive area in winter is half that in summer (Table 4).

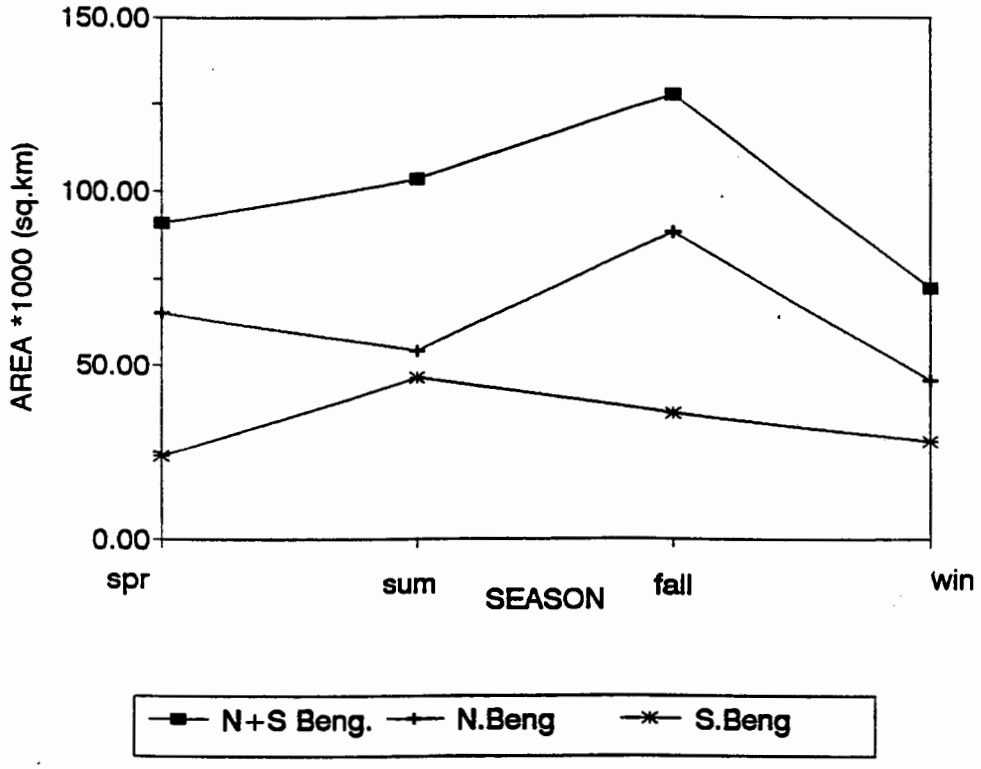

Figure 2. The Benguela productive area defined as that area with a mean pigment concentration of greater than 2mg m^{-3}. The seasonal variations in the magnitude of the productive area in both the northern and southern Benguela regions are synchronous with their mean pigment concentrations (see Figure 1).

The mean seasonal pigment concentration of the Benguela as a whole (1.8mg m^{-3}) was found to be 6.4 times that of the mean of the two Southern Ocean frontal regions (0.3mg m^{-3}) (Table 3), the Subtropical Convergence mean (0.4mg m^{-3}) in turn being twice that of the Subantarctic Front (0.2mg m^{-3}). Also, the seasonal time series (Figure 1c) shows that, in general, the seasonal variation within these frontal regions is less pronounced than that in the Benguela regions, although the chlorophyll signal in the Subtropical Convergence frontal region does exhibit a maximum in the fall followed by a minimum during the winter months. However, it must be noted that the area of the two frontal regions is much greater than that of the Benguela Upwelling region confined to the continental shelf (Table 2). Thus, it appears that any increase in pigment concentration in the Southern Ocean frontal regions is sustained over a vast area for an extended period of time.

3.2.2. Interannual Variability

The time series of interannual data (Table 5) shows a marked interannual variation in pigment concentration in the northern and southern Benguela regions, as well as in the Subtropical Convergence region. This data is based on the austral annual composites covering the seven year period from October 1978 to September 1985, the interannual variation being clearly seen in Plate 5. The annual composite for October 1978 to September 1979 (Plate 5a) shows relatively low chlorophyll concentration values in all regions, averaging around 1mg m^{-3}, 3mg m^{-3} and 0.5mg m^{-3} in the northern Benguela, southern Benguela and Subtropical Convergence regions, respectively. These values show a marked increase two years later in the 1980-1 annual composite (Plate 5b), particularly in the Subtropical Convergence region where the mean pigment concentrations (2 - 5mg m^{-3}) are now comparable to those found in the Benguela Upwelling region. The 1981-2 annual composite (Plate 5c) shows these values as being even further enhanced in the Benguela region, where cells with a mean pigment concentration in excess of 5mg m^{-3} are now found. On the other hand, the pigment concentrations in the

Subtropical Convergence region have now decreased to a mean value of about 1.5mg m^{-3}.

TABLE 5: INTERANNUAL VARIATIONS (ref. Plate 5).
Austral Annual Means: Oct 1978 - Sep 1985

CONTINENTAL SHELF REGIONS

NORTHERN BENGUELA

	Valid	Mean	s.d.
1978-1979	378	0.59	0.37
1979-1980	357	0.73	0.84
1980-1981	378	1.98	0.98
1981-1982	378	3.08	1.46
1982-1983	378	2.77	2.01
1983-1984	378	1.23	0.96
1984-1985	146	0.37	0.16

SOUTHERN BENGUELA

	Valid	Mean	s.d.
1978-1979	368	1.06	1.13
1979-1980	368	0.93	0.90
1980-1981	368	1.37	1.35
1981-1982	368	2.18	1.36
1982-1983	368	1.46	1.08
1983-1984	368	1.21	1.03
1984-1985	288	0.51	1.29

SOUTHERN OCEAN FRONTAL REGIONS

SUBTROPICAL CONVERGENCE

	Valid	Mean	s.d.
1978-1979	4392	0.21	0.05
1979-1980	4372	0.17	0.06
1980-1981	3472	1.01	1.40
1981-1982	4297	0.56	0.28
1982-1983	4373	0.48	0.18
1983-1984	2292	0.37	0.44
1984-1985	3112	0.19	0.09

SUBANTARCTIC FRONT

	Valid	Mean	s.d.
1978-1979	4340	0.14	0.06
1979-1980	4084	0.10	0.04
1980-1981	3359	0.29	0.27
1981-1982	3004	0.31	0.38
1982-1983	4375	0.24	0.08
1983-1984	1631	0.18	0.07
1984-1985	2057	0.11	0.06

NOTE: "Valid" is the minimum number of level-III bins having values between 0.04 and 34mg/m^3. This minimum number is 100 for the northern and southern Benguela regions, and 550 for the frontal regions.

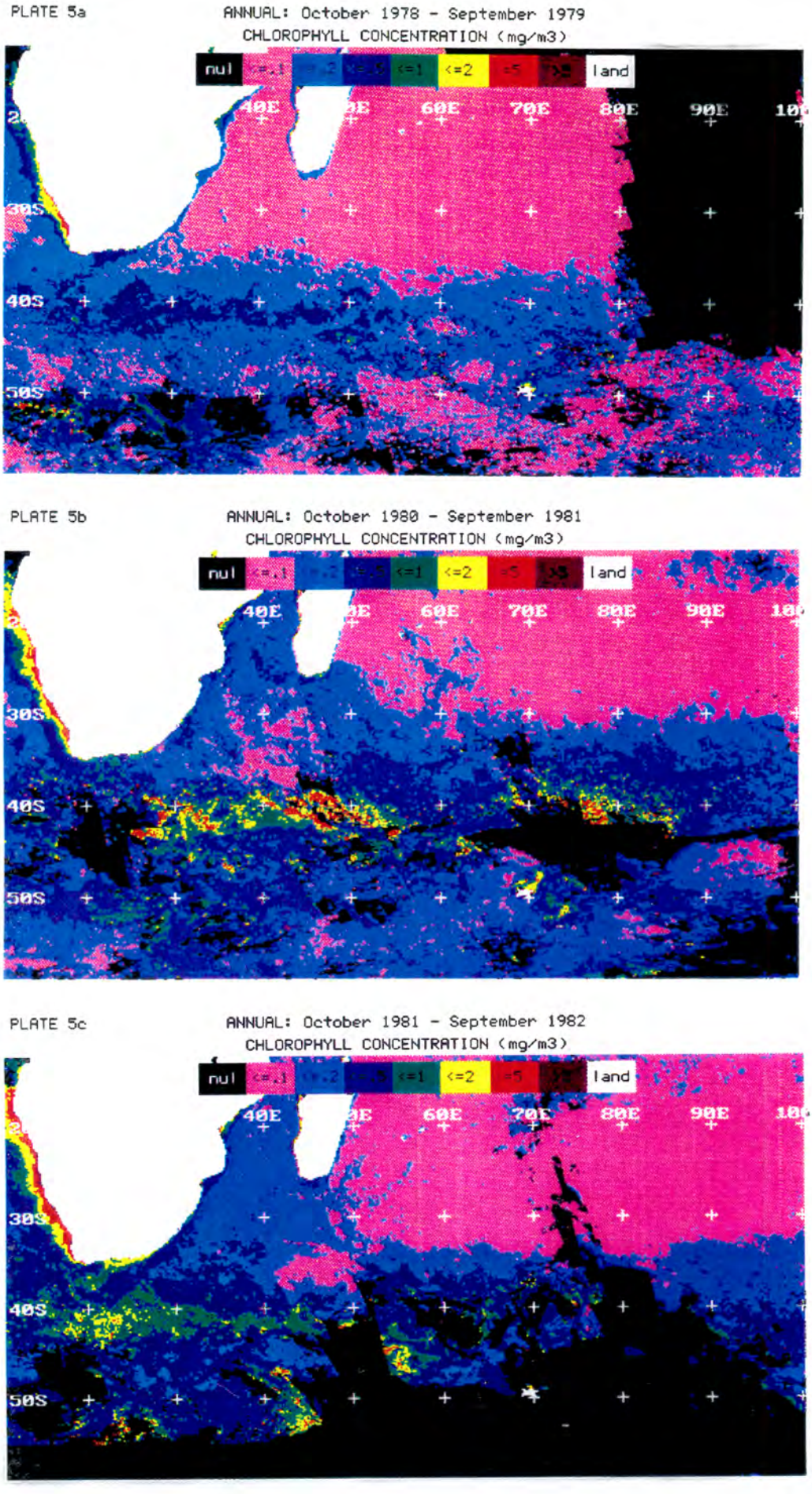

Plate 5. CZCS annual mean pigment concentrations for the austral years a) 1978-1979 b) 1980-1981 and c) 1981-1982.

The interannual means in Table 5 show some rather large standard deviations. However, there are problems in applying strict statistical tests to satellite images of geophysical data. This is because such data are spatially correlated and therefore not independent, also making it difficult to estimate degrees of freedom and standard errors [*Muller-Karger et al.*, 1991]. This problem is compounded by the fact that phytoplankton biomass is not distributed normally in space but rather follows a lognormal distribution [*Campbell and O'Reilly*, 1988]. So, in order to assess the interannual signal more accurately, the dataset was decomposed into individual seasons (Table 6). This intra-annual time series includes weighted interpolated means where data was too sparse, as described under "data analysis". The data was then filtered to remove the seasonal signal by applying a five-point weighted filter, the smoothing function weights being based on the equation: $c_m = N! / m!(N - m)!$ with $N = 4$, and $m = 0, 1, 2, 3$ and 4 [*Panofsky and Bier*, 1968]. The filtering process also had the effect of reducing individual seasonal means with excessive standard deviations to values closer to the mean intra-interannual value. The resulting intra- and interannual time series are shown in Figure 3.

The northern Benguela region (Figure 3a) exhibits the strongest interannual pigment signal with a minimum (0.6mg m^{-3}) in spring 1979, thereafter rising sharply during 1980 and remaining above 2.5mg m^{-3} before reaching a maximum (3.3mg m^{-3}) in fall 1982. The chlorophyll concentration remained above a mean of 2.5mg m^{-3} until fall 1983 after which it declined steadily for the remainder of the study period. Thus a five-fold interannual variation is observed. The southern Benguela interannual pigment signal (Figure 3a), while not as pronounced as that of the northern Benguela region, follows a similar trend, with a minimum (0.8mg m^{-3}) in spring 1979, rising to a maximum (2.2mg m^{-3}) in summer 1982 and then decreasing steadily for the remainder of the study period.

TABLE 6: INTRA- AND INTERANNUAL VARIATIONS. Seasonal Means: Spring 1978 - Winter 1985

CONTINENTAL SHELF REGIONS (ref. Figure 3a)

	NORTHERN BENGUELA			
	Valid	Mean	s.d.	Filtered Mean
SPRING 1978	143	3.28	4.14	1.54
SUMMER 1979	352	0.54	0.52	1.30
FALL 1979	378	0.79	0.52	0.82
WINTER 1979	342	0.60	0.48	0.62
SPRING 1979	335	0.55	0.63	0.55
SUMMER 1980	147	0.34	0.47	0.79
FALL 1980	302	0.92	1.19	1.74
WINTER 1980	127	4.29	4.73	2.76
SPRING 1980	143	3.28	4.14	2.89
SUMMER 1981	354	1.04	0.85	2.66
FALL 1981	378	4.24	2.42	2.77
WINTER 1981	378	2.10	1.19	2.82
SPRING 1981	290	2.92	1.88	2.85
SUMMER 1982	378	2.80	1.41	3.16
FALL 1982	378	4.41	2.61	3.26
WINTER 1982	65	2.26	0.74	2.96
SPRING 1982	33	2.47	0.88	2.81
SUMMER 1983	235	3.50	2.23	2.94
FALL 1983	378	2.79	2.16	2.85
WINTER 1983	191	2.61	2.87	2.41
SPRING 1983	0	1.80		1.86
SUMMER 1984	346	1.00	0.82	1.52
FALL 1984	373	1.69	1.74	1.54
WINTER 1984	0	1.76		1.58
SPRING 1984	0	1.64		1.31
SUMMER 1985	146	0.37	0.16	0.94
FALL 1985	0	0.91		0.97
WINTER 1985	0	0.95		0.74
	SOUTHERN BENGUELA			
	Valid	Mean	s.d.	Filtered Mean
SPRING 1978	363	1.20	1.42	1.41
SUMMER 1979	368	2.11	2.91	1.22
FALL 1979	368	0.93	0.81	1.16
WINTER 1979	368	0.65	0.59	0.86
SPRING 1979	368	0.76	0.73	0.78
SUMMER 1980	366	0.96	1.23	0.87
FALL 1980	308	0.61	0.82	1.12
WINTER 1980	366	2.12	2.40	1.39
SPRING 1980	363	1.20	1.42	1.47
SUMMER 1981	368	1.23	1.71	1.55
FALL 1981	368	2.29	2.05	1.75
WINTER 1981	368	1.45	1.21	1.92
SPRING 1981	368	2.35	1.62	2.10
SUMMER 1982	368	2.29	1.51	2.22
FALL 1982	341	2.30	1.39	2.08
WINTER 1982	24	1.62	0.17	1.77
SPRING 1982	368	1.41	0.88	1.57
SUMMER 1983	368	1.51	1.30	1.58
FALL 1983	368	1.88	1.32	1.64
WINTER 1983	368	1.56	1.87	1.53
SPRING 1983	281	1.22	1.36	1.36
SUMMER 1984	368	1.16	0.93	1.32
FALL 1984	368	1.64	1.72	1.30
WINTER 1984	0	1.16		1.03
SPRING 1984	197	0.35	0.37	0.62
SUMMER 1985	273	0.27	0.15	0.40
FALL 1985	9	0.43	0.39	0.41
WINTER 1985	112	0.80	0.37	0.43

TABLE 6 (continued)

SOUTHERN OPEN FRONTAL REGIONS (ref. Figure 3b)

	Valid	Mean	s.d.	Filtered Mean
SUBTROPICAL CONVERGENCE				
SPRING 1978	1872	0.47	0.96	0.32
SUMMER 1979	4215	0.23	0.10	0.29
FALL 1979	4377	0.27	0.13	0.25
WINTER 1979	4381	0.20	0.08	0.20
SPRING 1979	4354	0.15	0.04	0.17
SUMMER 1980	2104	0.13	0.07	0.18
FALL 1980	2691	0.23	0.21	0.24
WINTER 1980	1604	0.34	0.22	0.36
SPRING 1980	1872	0.47	0.96	0.58
SUMMER 1981	1653	0.80	1.39	0.91
FALL 1981	2212	1.77	1.63	1.04
WINTER 1981	98	0.39	0.68	0.83
SPRING 1981	3202	0.62	0.52	0.64
SUMMER 1982	4017	0.61	0.41	0.65
FALL 1982	1591	0.85	0.71	0.68
WINTER 1982	2011	0.55	0.74	0.62
SPRING 1982	4196	0.54	0.42	0.54
SUMMER 1983	4317	0.44	0.24	0.52
FALL 1983	3666	0.66	0.68	0.50
WINTER 1983	593	0.39	0.58	0.42
SPRING 1983	1008	0.21	0.15	0.35
SUMMER 1984	1236	0.41	0.48	0.39
FALL 1984	1418	0.57	1.08	0.43
WINTER 1984	0	0.34		0.36
SPRING 1984	1968	0.22	0.09	0.27
SUMMER 1985	2303	0.20	0.10	0.22
FALL 1985	70	0.20	0.02	0.20
WINTER 1985	2177	0.19	0.11	0.20
SUBANTARCTIC FRONT				
	Valid	Mean	s.d.	Filtered Mean
SPRING 1978	185	0.14	0.11	0.14
SUMMER 1979	2617	0.12	0.06	0.14
FALL 1979	3123	0.15	0.12	0.14
WINTER 1979	2710	0.17	0.13	0.14
SPRING 1979	3952	0.12	0.04	0.12
SUMMER 1980	2135	0.06	0.02	0.12
FALL 1980	0	0.16		0.16
WINTER 1980	200	0.25	0.14	0.22
SPRING 1980	185	0.25	0.11	0.26
SUMMER 1981	3177	0.28	0.36	0.28
FALL 1981	273	0.31	1.59	0.30
WINTER 1981	695	0.30	0.69	0.30
SPRING 1981	1203	0.27	0.30	0.29
SUMMER 1982	2193	0.29	0.37	0.29
FALL 1982	0	0.31		0.30
WINTER 1982	1700	0.32	0.42	0.29
SPRING 1982	3071	0.25	0.08	0.26
SUMMER 1983	3852	0.21	0.11	0.23
FALL 1983	167	0.24	0.31	0.22
WINTER 1983	0	0.22		0.21
SPRING 1983	1631	0.18	0.07	0.18
SUMMER 1984	0	0.14		0.16
FALL 1984	0	0.15		0.15
WINTER 1984	0	0.17		0.15
SPRING 1984	2253	0.12	0.04	0.13
SUMMER 1985	1704	0.11	0.08	0.12
FALL 1985	0	0.11		0.11
WINTER 1985	1038	0.10	0.04	0.11

NOTE: "Valid" is the minimum number of level-III bins having values between 0.04 and 34mg/m . This minimum number is 100 for the northern and southern Benguela regions, 550 for the frontal regions. "Mean" is replaced by an interpolated weighted mean when this condition is not met.

Figure 3a

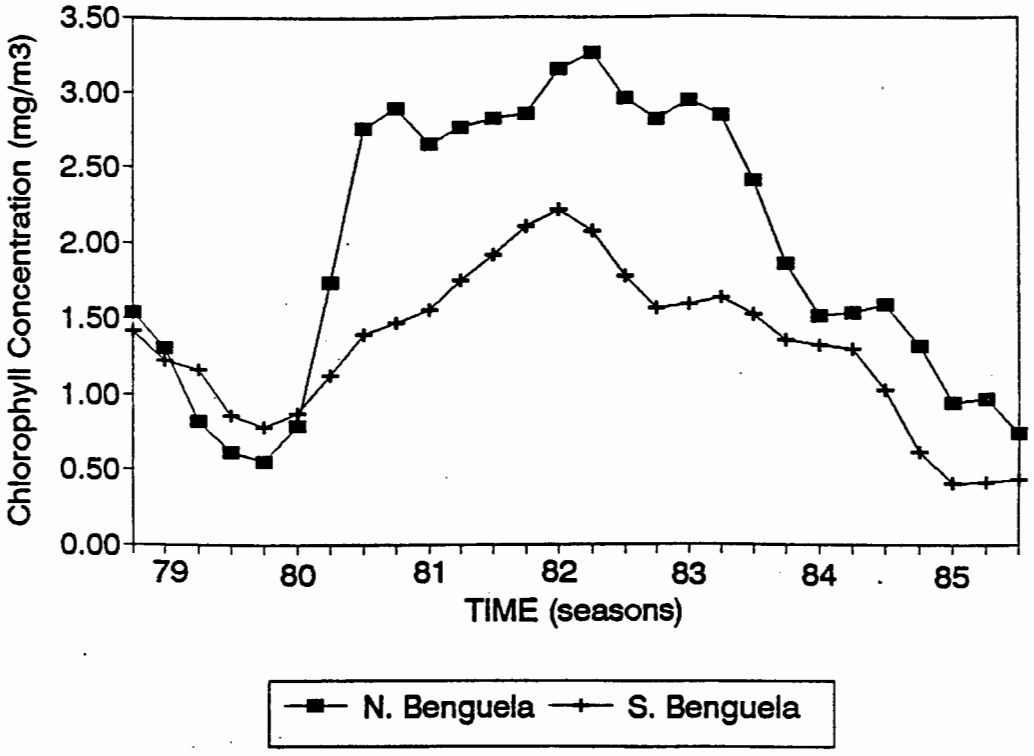

Figure 3b

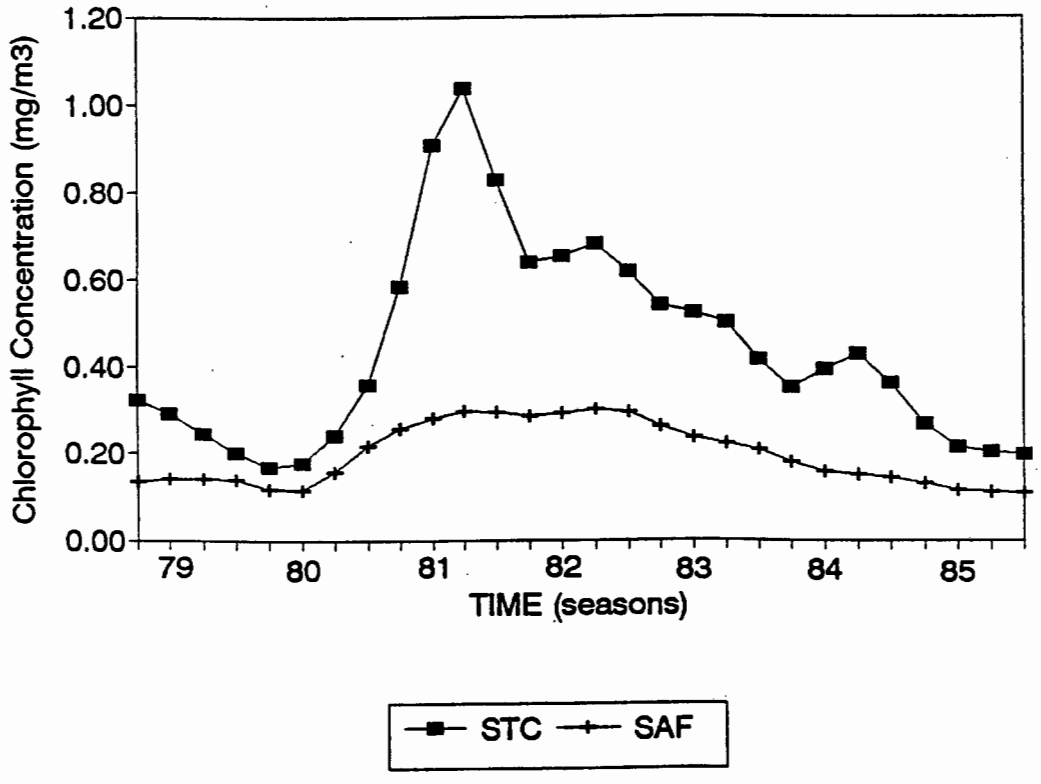

Figure 3. Interannual time series of mean seasonal pigment concentration for spring 1978 to winter 1985. The strongest interannual variation is in the northern Benguela (Figure 3a) with a maximum in fall 1982, while in the southern Benguela, there is a similar, although less pronounced, trend with a maximum in summer 1982. The Subtropical Convergence region (Figure 3b) shows a maximum in fall 1981, with no significant variation in the Subantarctic frontal region.

In contrast, the interannual pigment concentration in the Subtropical Convergence region (Figure 3b) has a low value (<0.4mg m^{-3}) throughout 1979 and most of 1980, rising sharply to a maximum (1.04mg m^{-3}) in the fall of 1981, and then decreasing again to reach values of less than 0.4mg m^{-3} in winter 1984 where it remained for the balance of the study period. This interannual mean pigment variation in the Subtropical Convergence region shows a totally different trend to that experienced in the Benguela regions, suggesting the influence of different physical forcing mechanisms. No significant interannual signal is seen in the Subantarctic Front region (Figure 3b).

Since the full CZCS statistical count dataset was unavailable and data paucity in the study area was a reason for concern, a comparative interannual time series analysis between the Subtropical Convergence zone and the monsoon region of the northwestern Arabian Sea was undertaken, both regions being subject to Indian Ocean easterly wind stress: during the southwestern monsoon period (June to September), surface-level southeasterly trades from the Southern Hemisphere extend across the equator to become the southwesterlies of the Northern Hemisphere [*Brock and McClain*, 1992]. The northwestern Arabian Sea region was also one of the areas more frequently sampled by the Nimbus-7 CZCS [*McClain et al.*, 1991]. The two regions were shown to both exhibit peaks in 1981 (Figure 4 and Plate 6), the northwestern Arabian Sea region reaching its maximum a season later (July to September) than the Subtropical Convergence region (April to June), coincident with the southwestern monsoon period. Thus, it would appear that two remotely distant regions with vastly different CZCS coverage, but subject to the same large scale oceanic physical forcing mechanism, exhibit similar interannual trends. This result lends credibility to the temporal trends obtained in this study from the CZCS data for the southern African region. This credibility is further reinforced by the marked interannual variation seen throughout the seven and a half year study period despite the fact that the frequency of data coverage differed considerably before and

after June 1981: 50% of the total CZCS scenes were acquired in the first 32 months out of a total CZCS lifetime of 92 months [*Feldman*, 1989].

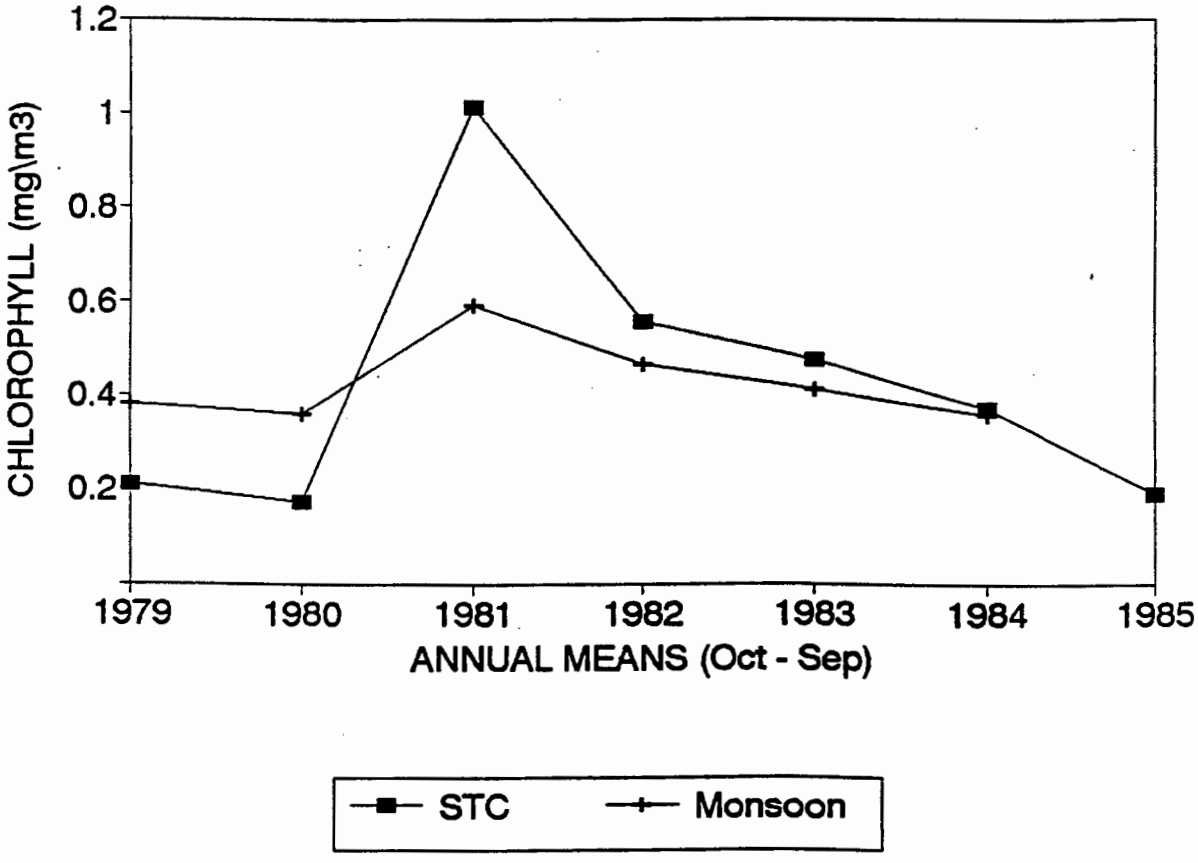

Figure 4. Interannual time series of mean annual pigment concentration for 1979 to 1985. Both the Subtropical Convergence and northwestern Arabian Sea monsoon regions exhibit peaks in 1981.

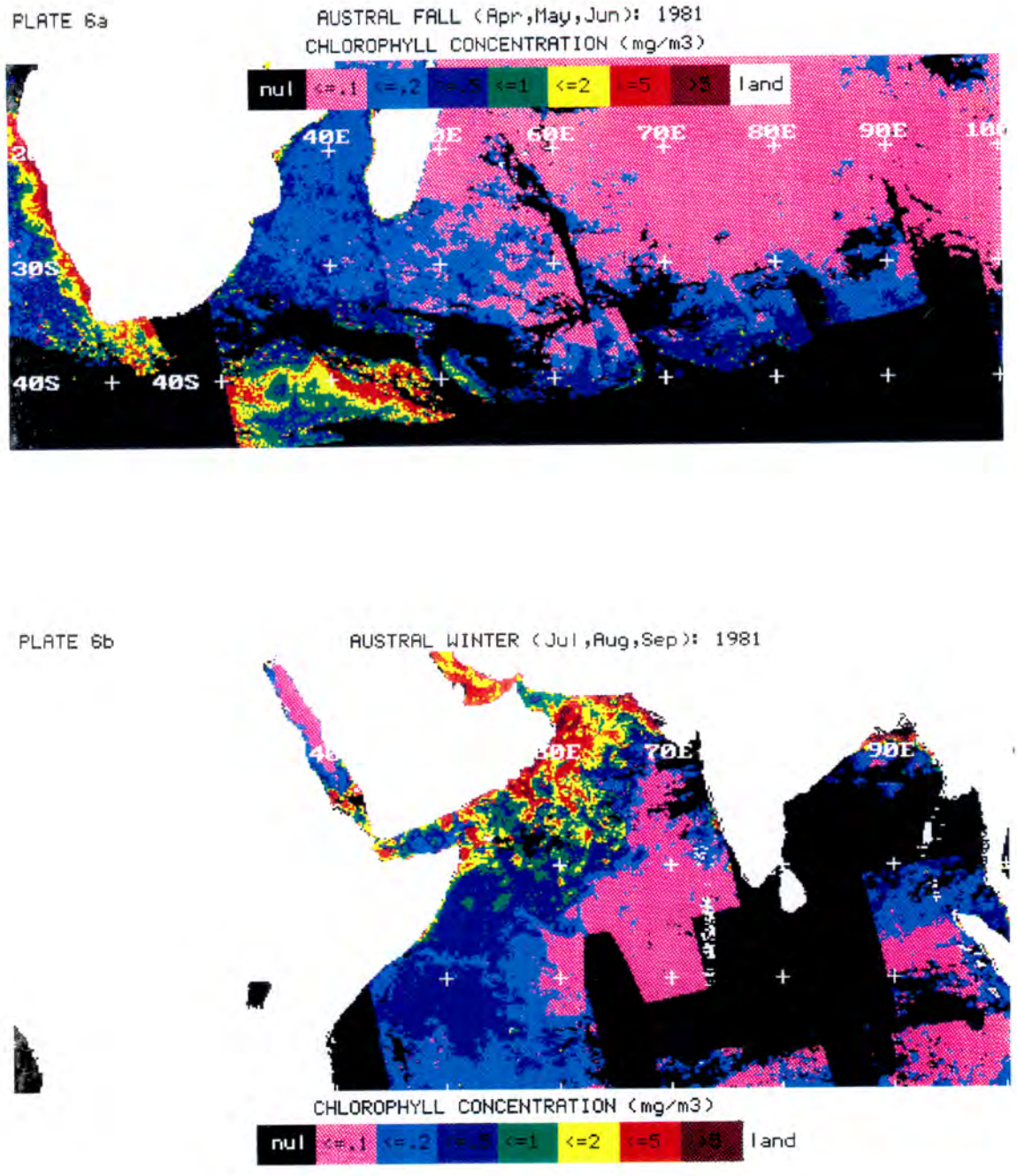

Plate 6. CZCS seasonal mean pigment concentrations for a) the Subtropical Convergence in austral fall 1981 and b) the northwestern Arabian Sea in austral winter 1981.

3.3. SEA SURFACE TEMPERATURE

Plate 7 clearly shows the seasonal sea surface temperature variability within the study area for the period including October 1981 to September 1982. Cells of cooler upwelled waters are seen in the Benguela Upwelling region and a seasonal meridional shift of the Subtropical Convergence front is clearly depicted in the contrasting mean summer and winter sea surface temperature images (Plates 7b and 7d). A warm eddy centred at 40^{o}S; 35^{o}E in the fall image (Plate 7c) appears to have persisted for much of the three month period, demonstrating the importance of cross-frontal eddies in the Subtropical Convergence region.

The corresponding mean seasonal pigment images for the same period are shown in Plate 8. The relative paucity of data in the study area is clearly demonstrated in this seasonal sequence, being especially sparse in the winter composite (Plate 8d), possibly due to increased cloud cover during this season. The four specific regions selected for detailed analysis (Table 2 and Plate 3) were delineated in both sets of images, the Benguela regions including that shelf area extending to the 500m isobath. However, a problem with the delineation of the Benguela regions arose due to the sea surface temperature data being obtained, already partially processed, from a different source to that of the CZCS and bathymetry datasets: the continental outline of the MCSST and CZCS images did not overlap accurately, being up to two pixels (about 35km) different at places. Similarly, the offshore topographic contours, generated from the U.S. Navy bathymetry dataset and corresponding to the CZCS data, were not accurate for the MCSST dataset. However, since bathymetry data corresponding to the MCSST dataset was not available, it was decided to continue with the analysis, bearing in mind that the results would probably be affected by the above shortcoming.

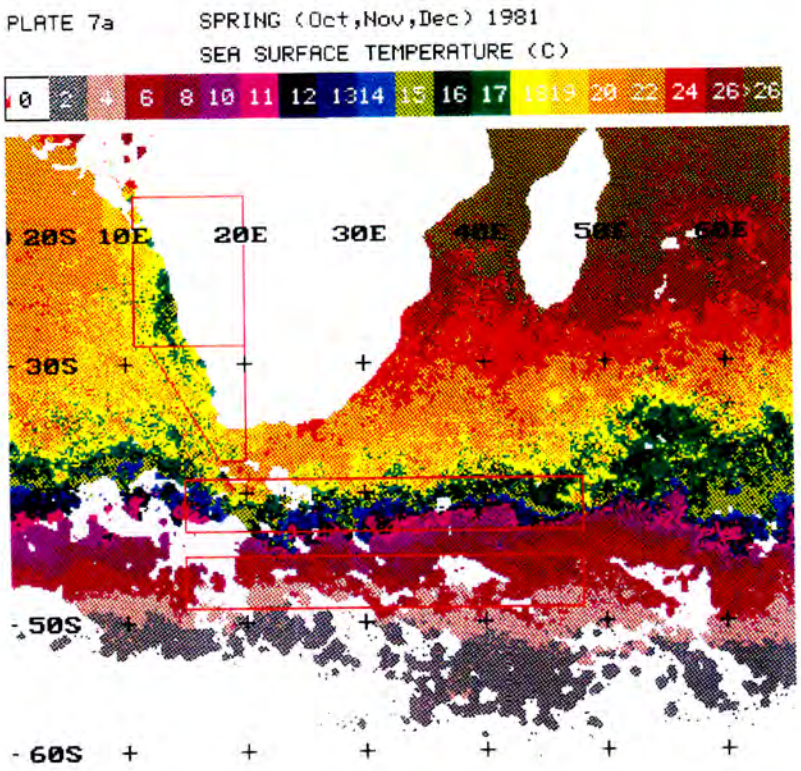

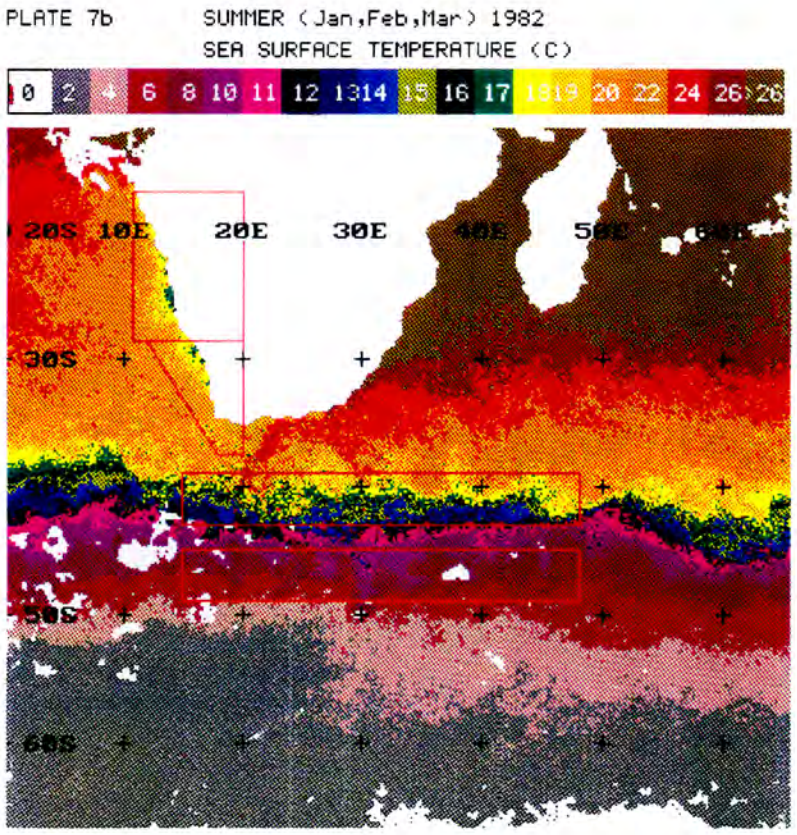

Plate 7. Seasonal mean sea surface temperatures for the austral seasons a) spring 1981 and b) summer 1982. Regions selected for detailed analysis are delineated.

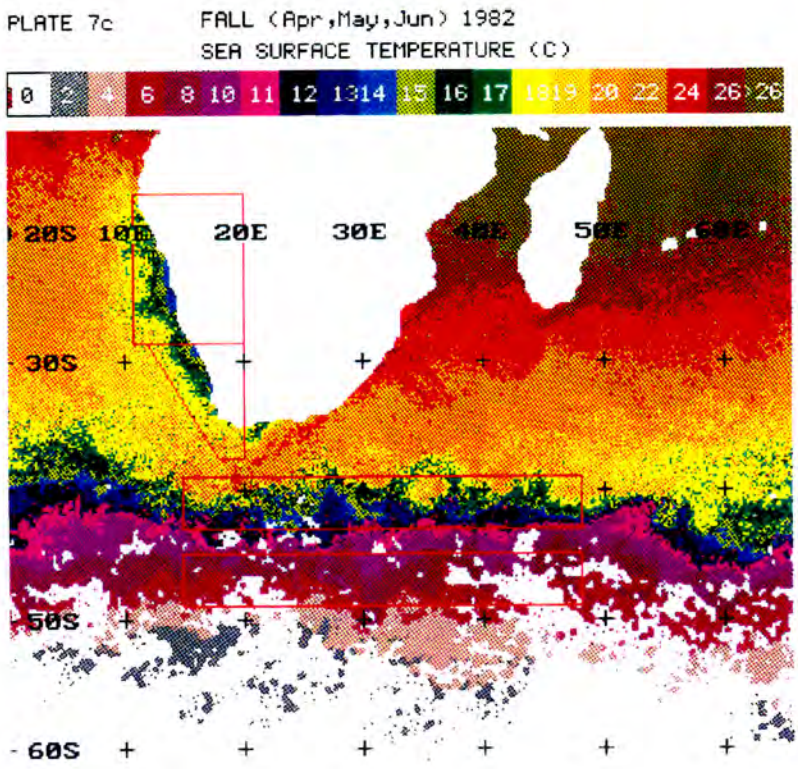

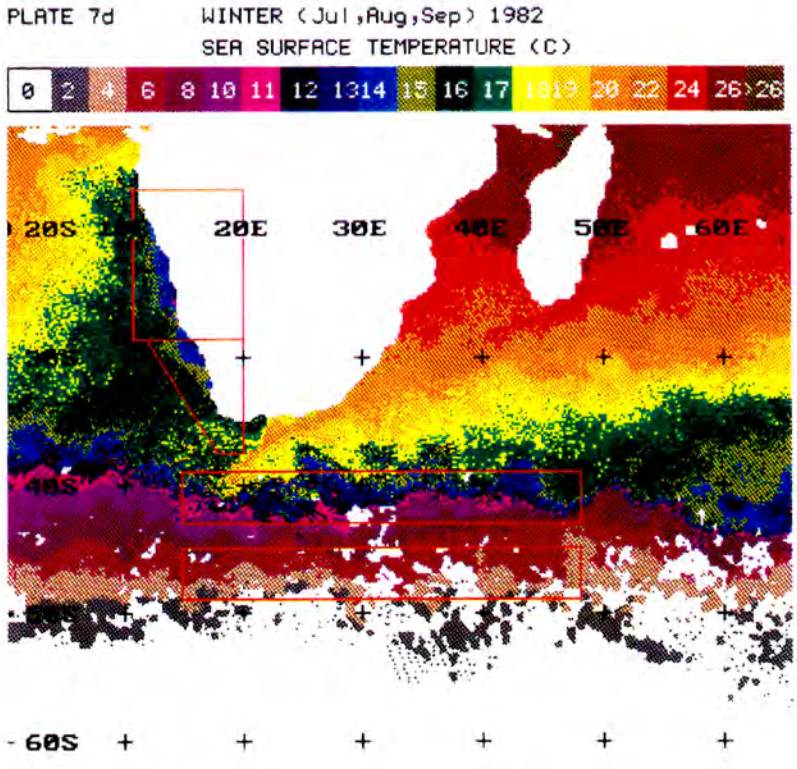

Plate 7 (continued). Seasonal mean sea surface temperatures for the austral seasons c) fall 1982 and d) winter 1982.

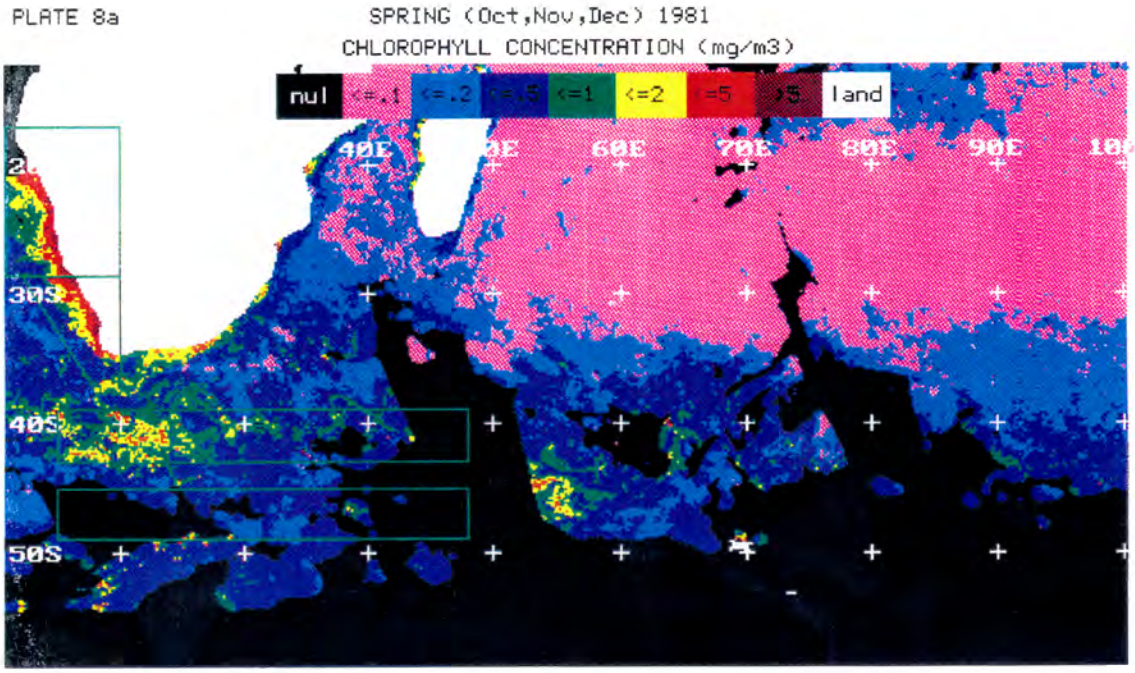

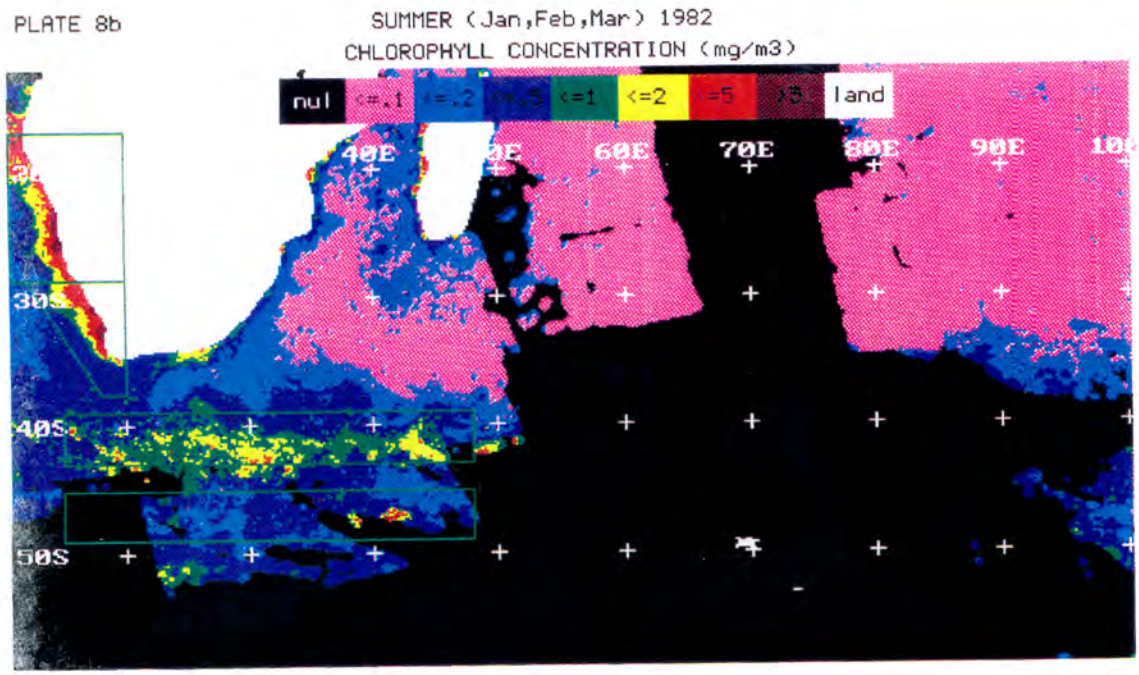

Plate 8. CZCS seasonal mean pigment concentrations for the austral seasons a) spring 1981 and b) summer 1982. Regions selected for detailed analysis are delineated.

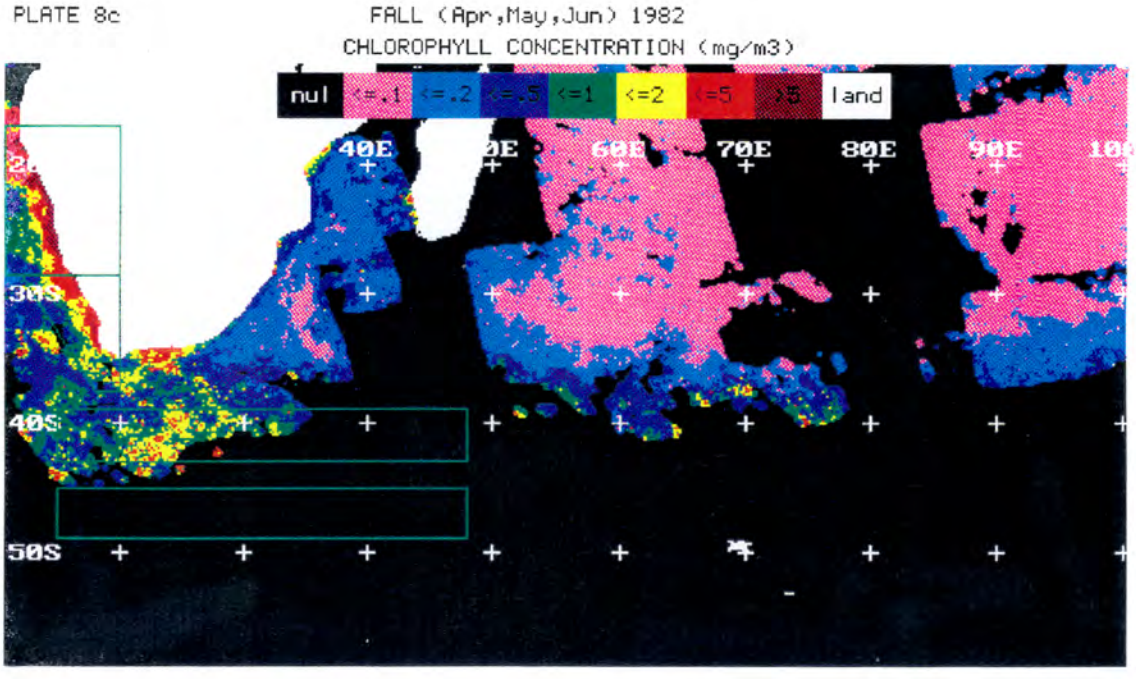

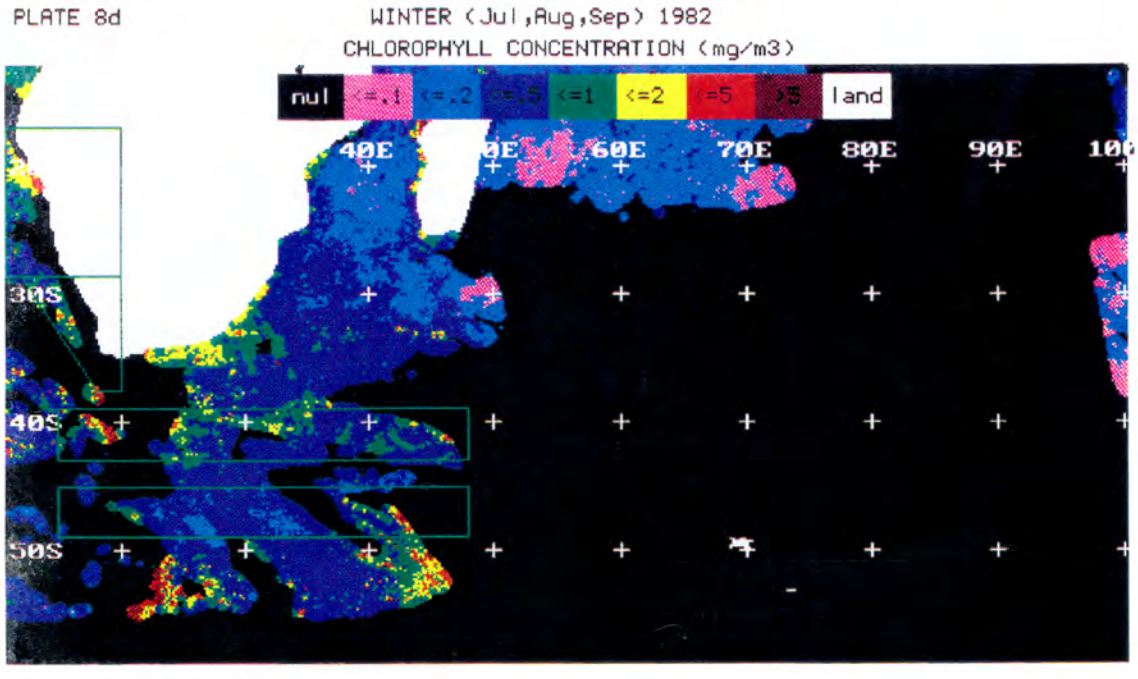

Plate 8 (continued). CZCS seasonal mean pigment concentrations for the austral seasons c) fall 1982 and d) winter 1982.

In order to assess the relationship between sea surface temperature and chlorophyll concentration, a seasonal times series of mean sea surface temperature was computed for the October 1981 to September 1982 period for the four selected regions (Table 7). The number of pixel values, mean sea surface temperature and standard deviation for each region and season are listed in Table 7a, along with the corresponding mean pigment concentrations. No filtering or interpolation has been applied to this data: in cases where the minimum number of "valid" CZCS values was not met, the data point was simply omitted from any further analysis, as occurred in the northern and southern Benguela regions during winter 1982, and in the Subantarctic region during fall 1982 (Table 7a). Thus, the scatterplot of sea surface temperature versus chlorophyll concentration shown in Figure 5 is based on thirteen sample values only. Regression analysis was applied to this data, resulting in a correlation coefficient of 0.64 (Table 7b). However, on examining Figure 5 and the data in Table 7a, it appeared that the Benguela Upwelling and Southern Ocean frontal regions should be regarded separately. Regression analyses were therefore applied to the two separate sets of data (Table 7b), correlation coefficients of -0.72 and 0.90 thus being obtained for the Benguela and frontal regions, respectively. Unfortunately, the number of samples in the two respective groups were only six and seven, thus limiting the significance of these results. Nonetheless, Table 7 does show that the highest mean seasonal pigment concentration in the Benguela regions (4.4mg m^{-3}) was obtained at a mean seasonal sea surface temperature of 15.0^{o}C, and in the frontal regions (0.85mg m^{-3}) at a mean sea surface temperature of 15.1^{o}C.

TABLE 7. SEA SURFACE TEMPERATURE AND CHLOROPHYLL VARIATIONS.
Seasonal means: Spring 1981 – Winter 1982
(ref. Plates 7 and 8, Figure 5)

TABLE 7a.

	SEA SURFACE TEMPERATURE			CHLOROPHYLL		
	Valid	Mean	s.d.	Valid	Mean	s.d.
NORTHERN BENGUELA						
SPRING 1981	232	16.66	1.06	290	2.92	1.88
SUMMER 1982	233	17.95	1.17	378	2.80	1.41
FALL 1982	273	15.01	1.40	378	4.41	2.81
WINTER 1982	280	13.65	1.41	Omitted		
SOUTHERN BENGUELA						
SPRING 1981	284	17.76	1.02	368	2.35	1.62
SUMMER 1982	284	18.64	1.32	368	2.29	1.51
FALL 1982	299	16.05	1.37	341	2.30	1.39
WINTER 1982	297	14.43	1.14	Omitted		
SUBTROPICAL CONVERGENCE						
SPRING 1981	3840	14.18	3.05	3202	0.62	0.52
SUMMER 1982	4214	16.19	2.91	4017	0.61	0.41
FALL 1982	4176	15.12	2.97	1591	0.85	0.71
WINTER 1982	4106	12.26	3.06	2011	0.55	0.74
SUBANTARCTIC FRONT						
SPRING 1981	3078	5.09	1.39	1203	0.27	0.30
SUMMER 1982	3936	6.78	1.42	2193	0.29	0.37
FALL 1982	3134	6.49	1.37	Omitted		
WINTER 1982	3126	4.10	1.33	1700	0.32	0.42

NOTE: "Valid" a) for SST: is the number of pixels having temperature values between 0 and 32°C.
b) for chlorophyll: is the number of level-III bins having values between 0.04 and 34mg/m³. If < 100 for Benguela regions, or < 500 for Frontal regions, the value is omitted.

Table 7b. Regression Analyses: Sea surface temperature and chlorophyll concentration.

	Above 4 regions	Benguela regions	Frontal regions
Constant	-0.73	10.18	0.1
X coefficient	0.17	-0.43	0.04
R squared	0.41	0.51	0.81
Correlation coefficient	0.64	-0.72	0.9
No. observations	13	6	7

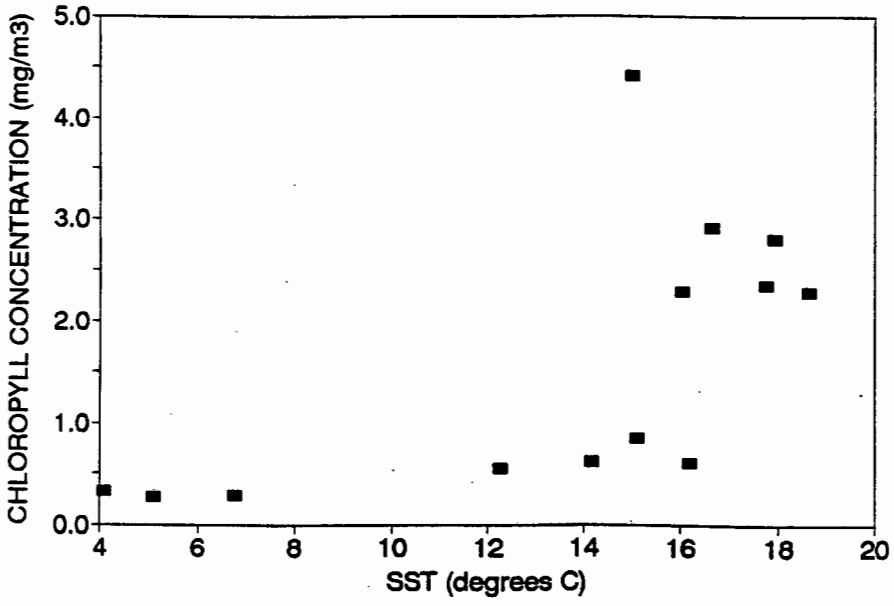

Figure 5. Scatterplot of seasonal mean sea surface temperatures and chlorophyll concentrations for spring 1981 to winter 1982 for the regions listed in Table 7.

Since it appeared that no significant statistical results could be obtained from the data in Table 7 due to the limited number of samples, the author decided to further decompose the data so as to obtain some understanding of the seasonal variability of sea surface temperature and chlorophyll in the Benguela shelf and oceanic (beyond the 500m isobath) substrata. Using the U.S. Navy bathymetry dataset, 0m, 200m, 500m 2000m and 4000m topographic contours were generated and overlain on the MCSST and CZCS images such that these data were decomposed into 0 to 200m, 200 to 500m, 500 to 2000m and 2000 to 4000m substrata. The inaccuracy of the topographic contours for the MCSST data was unfortunately highlighted by this data decomposition, especially in the inner shelf regions. Nonetheless, time series of mean seasonal sea surface temperature and chlorophyll were computed for each substratum. These values are listed in Table 8 and the seasonal variability for the 1981 to 1982 period is shown in Figure 6.

The seasonal sea surface temperature variability in the northern and southern Benguela regions follow the same trend, maximum and minimum temperatures being seen during the summer and winter months, respectively (Figures 6a and 6b). This variability is probably primarily due to the effects of insolation since the AVHRR measures "skin" temperature only. In both regions, the minimum temperatures are found in the most inshore substratum, increasing progressively offshore (Figures 6a and 6b), whereas the inverse occurs with the chlorophyll concentrations, maximum values being found inshore and decreasing progressively offshore (Figures 6c and 6d). This spatial distribution is consistent with intense coastal upwelling of cold, nutrient-rich waters, warmer, nutrient-poor waters being found in the deeper oceanic regions beyond the continental shelf. It could thus be expected that a regression analysis of these two datasets (Table 8) would reveal a strong negative correlation. However, a correlation coefficient of -0.16 only was obtained. This is probably mainly due to the inaccurate areal delineation of

TABLE 8. DECOMPOSED SEA SURFACE TEMPERATURE AND CHLOROPHYLL VARIATIONS
Seasonal means: Spring 1981–Winter 1982: 0–4000m depths (ref.Figure 6)

		SEA SURFACE TEMPERATURE			CHLOROPHYLL		
Substrata	Season	Valid	Mean	s.d.	Valid	Mean	s.d.
NORTHERN BENGUELA							
0–200m	SPRING 1981	188	16.62	1.06	201	4.42	2.00
	SUMMER 1982	185	17.81	1.19	253	3.98	1.38
	FALL 1982	223	14.83	1.39	253	6.25	2.84
	WINTER 1982	230	13.49	1.42	Omitted		
200–500m	SPRING 1981	238	17.16	0.99	243	2.73	1.88
	SUMMER 1982	263	18.79	0.99	312	2.64	1.39
	FALL 1982	266	16.13	1.19	310	3.93	2.49
	WINTER 1982	266	14.63	0.95	100	1.31	0.66
500–2000m	SPRING 1981	242	17.51	0.94	241	1.38	0.99
	SUMMER 1982	252	19.36	0.90	335	1.60	1.43
	FALL 1982	252	16.81	1.02	335	2.38	1.87
	WINTER 1982	252	15.18	0.75	202	0.81	0.39
2000–4000m	SPRING 1981	270	17.84	0.76	373	0.84	0.74
	SUMMER 1982	271	19.85	0.73	405	0.66	1.26
	FALL 1982	271	17.41	0.80	405	1.06	1.39
	WINTER 1982	271	15.84	0.53	280	0.50	0.20
SOUTHERN BENGUELA							
0–200m	SPRING 1981	243	17.76	1.04	221	3.53	1.83
	SUMMER 1982	243	18.52	1.36	221	3.39	1.77
	FALL 1982	258	15.91	1.40	218	2.91	1.61
	WINTER 1982	256	14.32	1.18	Omitted		
200–500m	SPRING 1981	191	17.89	1.13	271	1.97	1.25
	SUMMER 1982	192	19.68	0.81	271	2.05	1.39
	FALL 1982	195	17.32	0.94	265	1.97	1.11
	WINTER 1982	195	15.38	0.73	Omitted		
500–2000m	SPRING 1981	303	18.14	1.02	223	0.86	1.18
	SUMMER 1982	303	19.90	0.88	223	0.86	1.22
	FALL 1982	303	17.87	0.92	210	1.12	0.90
	WINTER 1982	303	15.67	0.73	133	0.75	0.71
2000–4000m	SPRING 1981	629	18.14	1.06	678	0.42	0.69
	SUMMER 1982	629	20.04	0.89	678	0.39	0.73
	FALL 1982	629	18.30	0.85	627	0.66	0.61
	WINTER 1982	629	15.94	0.72	180	0.73	0.71

NOTE: "Valid" a) for SST: is the number of pixels having temperature values between 0 and 32°C.
b) for chlorophyll: is the number of level-III bins having values between 0.04 and 34mg/m . If < 100, the value is omiited.

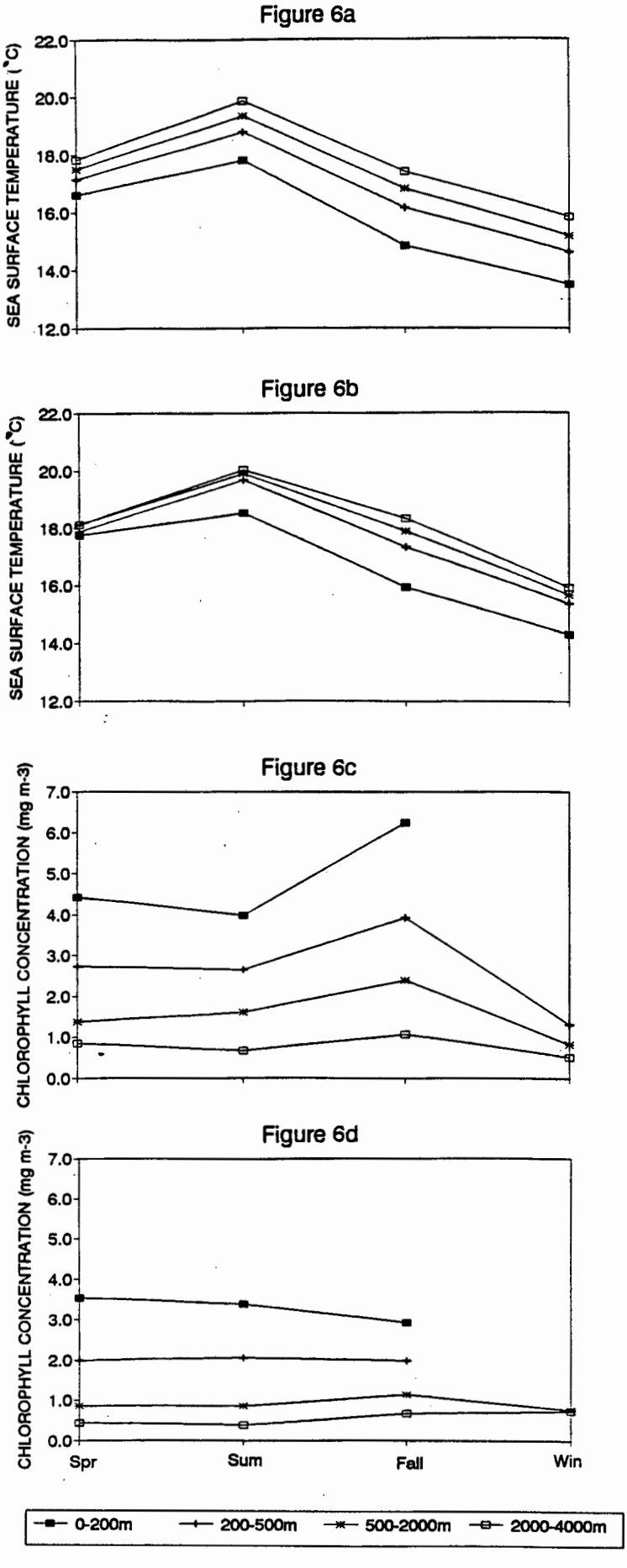

Figure 6. Seasonal mean sea surface temperatures for the a) northern Benguela and b) southern Benguela, and seasonal mean pigment concentrations for the c) northern Benguela and d) southern Benguela shelf and oceanic substrata for the period spring 1981 to winter 1982.

offshore substrata in the MCSST imagery, but may also be due to the fact that the data covers a wide range of sea surface temperature (13.5°C to 20.1°C) and chlorophyll (0.4mg m^{-3} to 6.25mg m^{-3}) values (Table 8), including both upwelled continental shelf waters and oceanic waters. Unless a direct linear relationship exists between these two parameters over this entire range, a strong correlation would not be obtained. This is borne out by the fact that the maximum mean seasonal chlorophyll concentration (6.3mg m^{-3}) in Table 8 is found at a mean seasonal sea surface temperature of 14.8°C, with lower chlorophyll concentrations found at both higher and lower sea surface temperatures. Also, maximum and minimum mean sea surface temperatures are seen during summer and winter, respectively, in both northern and southern Benguela regions (Figures 6a and 6b), whereas maximum mean chlorophyll concentrations are shown to occur during the fall months in the northern Benguela (Figure 6c), while similar mean chlorophyll concentrations are seen during spring, summer and fall in the southern Benguela shelf substrata despite an almost 3°C range in mean sea surface temperature (Figure 6d).

The data in Tables 7 and 8 and Figures 5 and 6, although limited, would suggest a positive correlation between mean seasonal sea surface temperature and mean seasonal chlorophyll concentration up to about 14°C, perhaps forming a temperature window between about 14°C and 17°C where maximum mean chlorophyll concentrations are achieved, and thereafter, a negative correlation between mean sea surface temperature and mean chlorophyll concentration.

Finally, since the above seasonal time series show sea surface temperature and chlorophyll mean values only, spatial correlations between the two parameters were computed for the full northern and southern Benguela regions delineated in Plates 7 and 8 (excluding land), for the spring, summer and fall 1981-2 seasons, winter data being too sparse. The area of the southern Benguela region was delineated to include similar offshore depths to that of the northern Benguela area

(Plates 7 and 8), the western limit being taken as 12°E in the north extending to intercept 37.5°S at 18°E in the south. The results of the spatial correlations are shown in Table 9 and Figure 7, maximum correlation coefficients being obtained during summer in both the northern Benguela (-0.6) and southern Benguela (-0.7) regions. However, the differing continental outline of the two sets of images once again created a problem, as seen from the number of sea surface temperature versus chlorophyll pixels per area in the scatterplots (Figure 7), and the number of pixels which actually overlapped and were used to compute the correlation coefficients in Table 9. The spatial analyses were therefore not pursued further in this study, and are merely noted as a technique for future use and for data processed from the initial digital stage.

TABLE 9. SPATIAL CORRELATIONS : SEA SURFACE TEMPERATURE vs CHLOROPHYLL. (ref. Figure 7)

	Pixels	Correlation coefficient
NORTHERN BENGUELA		
SPRING 1981	913	-0.41
SUMMER 1982	1065	-0.61
FALL 1982	1093	-0.54
WINTER 1982	—	
SOUTHERN BENGUELA		
SPRING 1981	951	-0.22
SUMMER 1982	949	-0.68
FALL 1982	905	-0.65
WINTER 1982	—	

NOTE: "Pixels" is the number of corresponding sea surface temperature and chlorophyll concentration pixels used to compute the correlation coefficient.

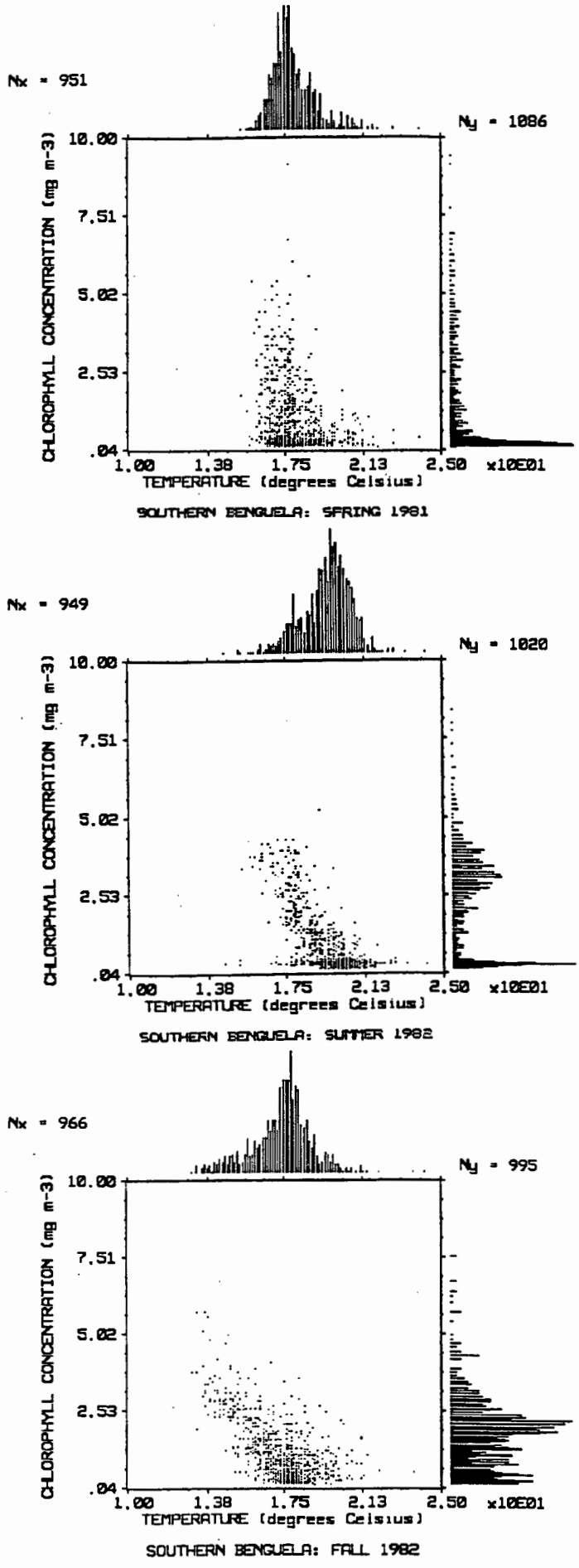

Figure 7. Scatterplots to determine the spatial correlations (Table 9) between seasonal mean sea surface temperature and pigment concentration for the southern Benguela for a) spring 1981 b) summer 1982 and c) fall 1982.

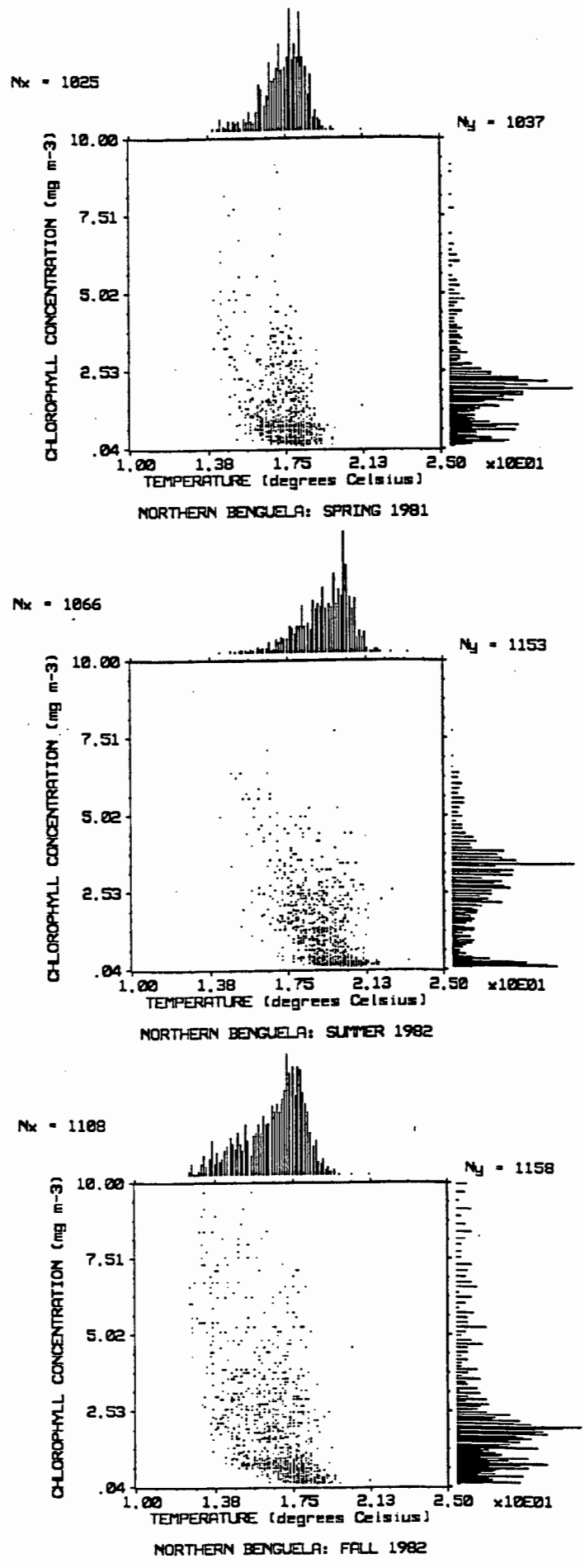

Figure 7 (continued). Scatterplots to determine the spatial correlations (Table 9) between seasonal mean sea surface temperature and pigment concentration for the northern Benguela for d) spring 1981 e) summer 1982 and f) fall 1982.

3.4. THE TOPOGRAPHIC ROSSBY WAVE

In order to resolve the Rossby wave seen in the Agulhas Return Current (Plate 2), a series of individual CZCS level-II scenes in which this feature was identified, were selected. Five of these CZCS scenes were then merged to form a level-II composite with a 4km resolution for the period 5 to 15 February 1983 (Plate 9a). Using the U.S. Navy bathymetry dataset, topographic contours for the same area as Plate 9a were generated, and overlain on the CZCS image. The sea surface temperature image for the corresponding period and area was extracted from the MCSST dataset and is shown in Plate 9b.

Plate 9a clearly shows the increased chlorophyll signal of the Subtropical Convergence front. The Agulhas Current is seen to leave the continental shelf at about 36^{o}S, thereafter continuing in a southerly direction before retroflecting to flow eastwards along the Subtropical Convergence, as the Agulhas Return Current. This eastward-flowing current, describes a series of meanders which appear to coincide with the bottom topography of the Agulhas Plateau and the Madagascar Ridge. A southward trend to this wave was also noted. The average wavelengths of the meanders in Plate 9 were 440km, with an average amplitude, or meridional excursion, of 330km.

If the Agulhas Return Current were to be regarded as a Rossby wave, then the wavelength may be determined from the equation: $\lambda = 2\pi\,(u/\beta)^{1/2}$, where u is the current speed and ß is the change in the Coriolis parameter, $f = 2\Omega\sin\Theta$ with latitude, with no limitation on the size of the wave amplitude [*Pedlosky*, 1987]. This results in a wavelength of 470km, if u, the vertically-integrated speed of the Agulhas Return Current is $O(10^{-1}ms^{-1})$ and ß, df/dy, is calculated for latitudes 37^{o}S and 40^{o}S. This wavelength is similar to that seen in Plate 9, suggesting that it is largely determined by ß-generated anticyclonic relative vorticity, which is

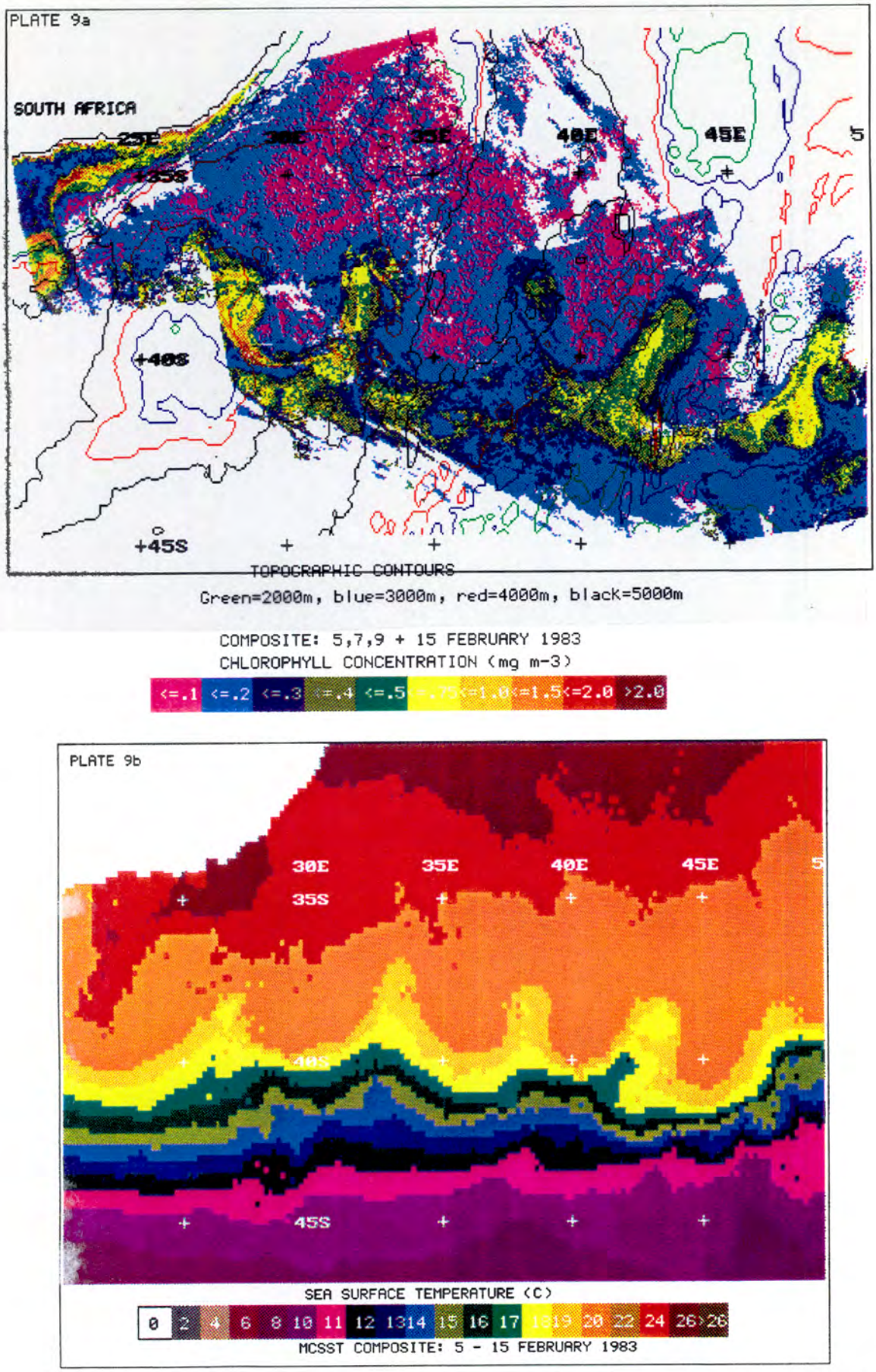

Plate 9. Plate 9a) CZCS composite of 5, 7, 9 and 15 February 1983 of the Rossby wave in the Agulhas Return Current, overlain by the topographic contours for the area. Plate 9b) Mean sea surface temperature for the period and area corresponding to Plate 9a.

accumulated as the Agulhas Current follows its southward path after having left the continental shelf at around 36^{o}S.

On retroflecting, however, the eastward-flowing Agulhas Return Current is almost immediately subjected to a considerable change in bottom topography as it encounters the Agulhas Plateau (Plate 9a). Using conservation of potential vorticity in this region [*de Ruijter*, 1982], an adjustment of the current flow to this topographic feature would be expected i.e. $\frac{d}{dt}\left(\frac{\zeta + f}{h}\right) = 0$, is maintained. Net positive relative vorticity (ζ) adjusts the flow in an anticyclonic manner to follow the topographic contours. This flow adjustment to the topographic contours is expected to take on a similar length scale to that of the slope of the topography. Now, λ has a scale of $O(U/L)$ for Rossby waves [*Pedlosky*, 1987] and, for a zonal current which experiences a relative change in depth, may be determined from the expression: $\zeta = f * h_2\text{-}h_1/h_1 *$ slope of the topography ($\blacktriangle h$), where h_1 and h_2 are the respective depths before and after the change in bottom topography [*Gill*, 1982]. Therefore, it follows that the length scale, L, due to the change in depth, may be estimated as: $L = U/f * h_1/\blacktriangle h(h_2\text{-}h_1)$. For a vertically-integrated current speed $O(0.1\text{m s}^{-1})$, Coriolis parameter $O(\text{-}10^{-4})$ and a change in depth from 5000m to 3000m over a distance of about 100km (Plate 9a), L is estimated to be O(100km). The flow response to the change in bottom topography is thus accomplished very rapidly.

The now northward-flowing current is subjected to the ß-effect, the net accumulated negative relative vorticity eventually dominating the flow, and effecting cyclonic curvature. The resulting eastward flow once again encounters a change in depth as it flows off the Agulhas Plateau, adjusting accordingly in a cyclonic manner to align itself with the topographic contours. The subsequent accumulation of ß-generated anticyclonic vorticity eventually again dominates, such that the flow 'breaks away' from the topographic feature, continuing eastwards as a Rossby wave, the shape of

the meridional excursions having been determined by the topographic contours. This flow pattern is clearly shown in Plate 9, where the Rossby wave, initiated in the retroflection area and then constrained by the Agulhas Plateau, continues eastwards with meridional excursions, the shape of which is further constrained to align with the topographic contours of the Madagascar Ridge, which it encounters downstream.

The Agulhas Current thus appears to follow contours of $^{f}/_{h}$ [*Gill and Parker*, 1970]. The contours of $^{f}/_{h}$, or h cosec Θ (Θ = latitude), are presented in Figure 8 for the area of interest to this study. Both the southward trend (10^{o}) of the Rossby wave in Plate 9, and the distance (1500km) between the peaks overlying the Agulhas Plateau and the Madagascar Ridge, are similar to points (A) and (B) in Figure 8. We therefore suggest that the Agulhas Current attempts to follow the contour, h cosec Θ = 6, where $^{f}/_{h} = {}^{2\Omega}/_{6}$ km and Ω is the rate of rotation of the earth. The importance of contours of $^{f}/_{h}$ for oceanic motion is an extensive subject however, with only a cursory exploration undertaken in this study.

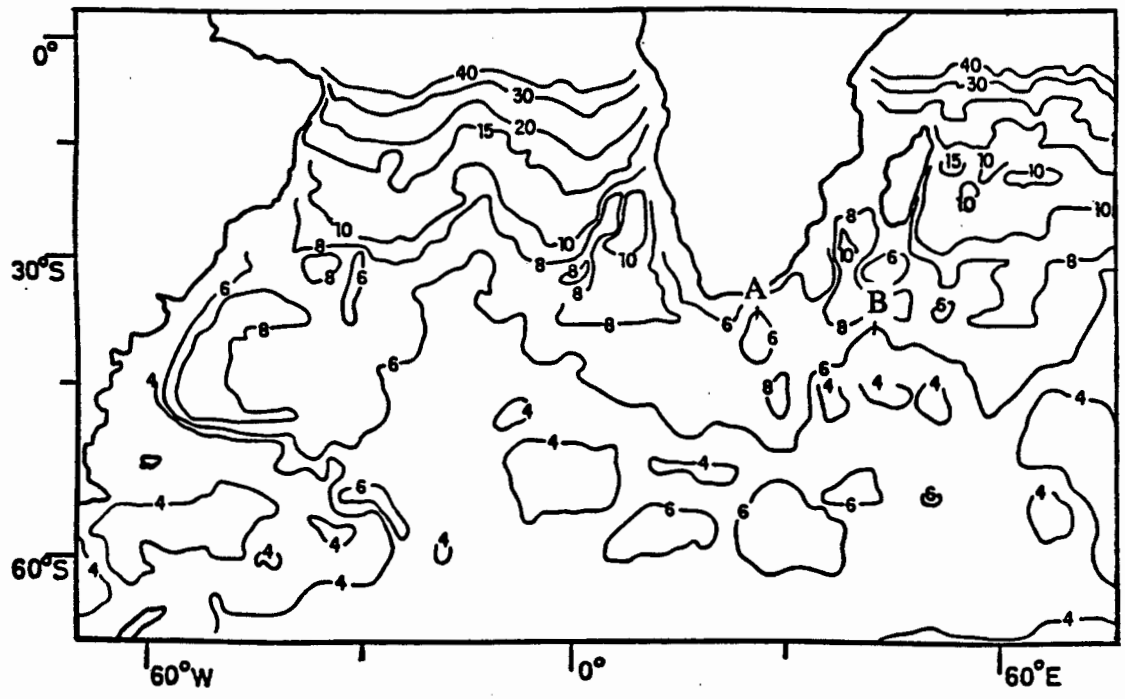

Figure 8. Contours of d = h cosec Θ (km) for the area of interest, drawn on a Mercator projection. (after *Gill and Parker*, 1970).

CHAPTER 4

DISCUSSION

The productive Benguela Upwelling system and the Subtropical Convergence region are potentially important carbon dioxide sinks in the Southern Hemisphere. Comparison of the Subtropical Convergence region with the Benguela Upwelling region shows that, although the mean pigment concentration of the former (1.8mg m^{-3}) is 5 times that of the latter (0.4mg m^{-3}) (Table 3), the area of the Subtropical Convergence region is 5 times that of the Benguela region (Table 2). Thus, the large expanse of the open ocean frontal region of the Subtropical Convergence can sustain a standing stock of phytoplankton over extended periods of time that is similar in magnitude to the phytoplankton standing stock in the Benguela region confined to the continental shelf.

The Benguela Upwelling system is "characterised by cyclonic wind-stress curl near the continental boundaries and anticyclonic curl offshore, in association with predominantly equatorward (upwelling favourable) alongshore wind stress" [*Bakun and Nelson*, 1991]. However, there are two distinct regimes in the Benguela Upwelling system. The southerly region experiences a clear seasonal wind-driven upwelling pattern which is strongest in the spring and summer, whereas upwelling in the northern Benguela region is more perennial [*Shannon et al.*, 1986; *Pearce*, 1991]. This is explained by the coastal area of cyclonic windstress curl appearing as a wedge extending from around 20°S, narrowing in offshore extent towards the south. The wedge has its most limited poleward extent in austral winter, when it reaches about 27°S. By early spring the wedge extends to about 33°S and beyond Cape Point by late spring, where it remains until it retreats northwards again during late fall [*Bakun and Nelson*, 1991]. Equatorward of 20°S, the distributions are less distinct.

In the southern Benguela, therefore, upwelling is most intense when the equatorwards wind stress is strongest, in the summer. This is due to the ridging of the South Atlantic high-pressure cell around the continent. In the north, the main upwelling period extends from March to November, although some upwelling takes place throughout the year [*Shannon*, 1985b] Also, a regular southwards intrusion of warm Angolan water occurs during the first quarter of each year (summer) [*Shannon, Lutjeharms and Nelson*, 1990] as the Angolan-Benguela front migrates southwards (Figure 9). This coincides with the partial relaxation in equatorward wind stress in the northern Benguela and a reduction in upwelling of nutrient-rich water to the surface (Figure 9). The seasonal variations of pigment concentration within these two regions (Figures 1a and 1b) have clearly been shown to be similarly out of phase, the maximum pigment concentrations being observed during the strongest upwelling periods.

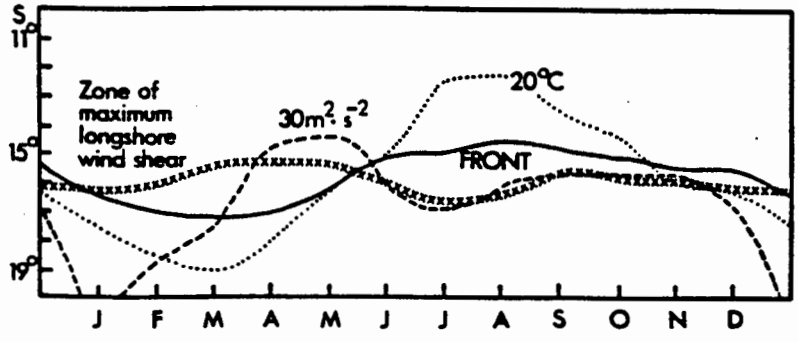

Figure 9. Monthly mean positions of the 20°C surface isotherm, the Angola-Benguela front and the $30m^2s^{-2}$ isopleth of wind speed squared near the coast for 1964 - 1979 (after *Shannon, Lutjeharms and Nelson*, 1990).

The mean pigment concentrations of the inner shelf substrata were shown to be greater than those of the outer shelf substrata in both the northern and southern Benguela regions (Table 3). *Brown* [1992] found similar results from shipboard measurements, also showing that the spatial distribution of chlorophyll is consistent with local upwelling patterns and concluded that this clear onshore offshore gradient

is due mainly to the coastal upwelling of nutrient-rich waters fueling phytoplankton close to the shore. *Brown and Cochrane* [1991] suggest that upwelling, by way of high nutrient concentrations in upwelled water, is more important that temperature in controlling chlorophyll concentration, although temperature influences the rate of primary production over a limited temperature range.

Analysis of the mean seasonal sea surface temperatures and mean seasonal chlorophyll concentrations for the austral year October 1981 to September 1982, although limited, suggests that the relationship between these two parameters takes the form of an inverted parabola, the interval about the maximum representing a temperature window of about 14 to 17^{o}C within which maximum chlorophyll concentrations are found. The highest mean chlorophyll concentrations in both the northern and southern Benguela regions were found at a mean sea surface temperature of around 15^{o}C. *Mitchell-Innes and Pitcher* [1992], whose study included the West coast shelf area over a wide spectrum of conditions, found an abrupt change in phytoplankton population composition at about 15^{o}C and propose that this was governed by the "attainment of a critical combination of nutrient, temperature and stability thresholds, rather than a temperature threshold per se". These authors showed a dome-shaped relationship between sea surface temperature and biomass, sea surface temperatures of 12 to 15^{o}C generally associated with high ($>$ 3mg m^{-3}) chlorophyll concentrations and diatom-dominated populations, whereas low ($<$ 3mg m^{-3}) chlorophyll concentrations and flagellate-dominated populations occurred below 12^{o}C and above 15^{o}C. They add that the upper and lower thresholds of this temperature window are likely to vary by a few degrees.

The limitations of the October 1981 to September 1982 sea surface temperature and chlorophyll data used in this study must be borne in mind: the sea surface temperature data represents surface "skin" temperature only, whereas the chlorophyll data represents the weighted mean concentrations over the first optical (attenuation) depth (*C. McClain*, pers. comm.). The time series analyses of the two

parameters (Tables 7 and 8) dealt with mean values for each season and region. Since no interpolated values were included and sea surface temperature fields were obtained for each week within the study period, the sea surface temperature composite values represent true seasonal means, whereas the number of CZCS values binned within each seasonal composite was probably considerably less, as indicated by the paucity of data (Plate 8). Without having access to the full CZCS statistical count dataset, one cannot ascertain whether the seasonal CZCS images represent the true CZCS seasonal means. In addition, the year 1982 has been shown to be anomalous [*Gillooly and Walker,* 1984; *Shannon et al.*, 1986; *Taunton-Clark*, 1990], the seasonal means therefore probably not representing true seasonal means for the Benguela regions. The above, together with the fact that *Mitchell-Innes and Pitcher* [1992] studied individual upwelling events rather than seasonal mean data, probably accounts for the difference in "temperature windows" found in the two studies. The author therefore suggests that future analyses of the sea surface temperature chlorophyll concentration relationship should both cover a longer time period and the temporal resolution should be such that individual upwelling pulses are resolved.

The average productive area (mean pigment concentration $> 2mg\ m^{-3}$) as a percentage of total area in the northern Benguela was found to be 1.7 times that of the southern Benguela (Table 4) inferring that the increased mean pigment concentration in the northern Benguela region is primarily due to a greater productive area, and not due to significantly higher pigment concentrations occurring within that region. Since chlorophyll concentrations of greater than $2mg\ m^{-3}$ may be roughly equated with diatom-dominated communities and concentrations of less than $2mg\ m^{-3}$ with micro-flagellates [*Mitchell-Innes and Walker*, 1991], the variation in the chlorophyll distribution (productive area), and hence phytoplankton production, may be used to monitor the structure of the ecosystem. *Brown and Cochrane* [1991] suggest that this could provide a regional

index, both of the food environment of pelagic fisheries and of the degree to which phytoplankton may constitute a carbon sink.

Pronounced interannual variation of pigment concentration has been shown during the study period, with chlorophyll maxima in fall 1982 and summer 1982 in the northern and southern regions, respectively. These coincide with the well-documented 1982-3 El-Nino Southern Oscillation event, when anomalous oceanographic and climatic conditions prevailed over southern Africa [*Gillooly and Walker*, 1984]. Upwelling favourable winds were lighter than normal during the years 1982 to 1983 [*Shannon et al*, 1986; *Taunton-Clark*, 1990], and a negative zonal wind anomaly was clearly seen in the equatorial Atlantic (Figure 10) [*Shannon, Lutjeharms and Nelson*, 1990]. However, the shelf and oceanic areas were distinctly out of phase during this period with below normal sea surface temperatures being found on the continental shelf from Cape to Namibia (Figure 11). The 1982-3 cool event has been described as due to enhanced coastal upwelling, although no matching increase in equatorward pseudo-wind stress was seen [*Taunton-Clark*, 1990], and is confirmed by the negative sea level anomalies seen in Figure 10. This perturbation was confined to the shelf area [*Shannon, Lutjeharms and Nelson*, 1990; *Taunton-Clark*, 1990], with the 1982-3 period being described as an extended period of vigorous upwelling [*Shannon et al*, 1986].

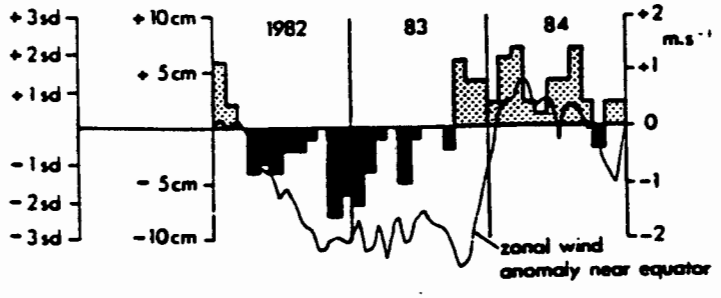

Figure 10. Anomalies in the mean monthly sea level adjusted for atmospheric pressure at Walvis Bay, and the 850-mb zonal wind anomalies for the equatorial Atlantic: 1982-1984 (after *Shannon, Lutjeharms and Nelson*, 1990).

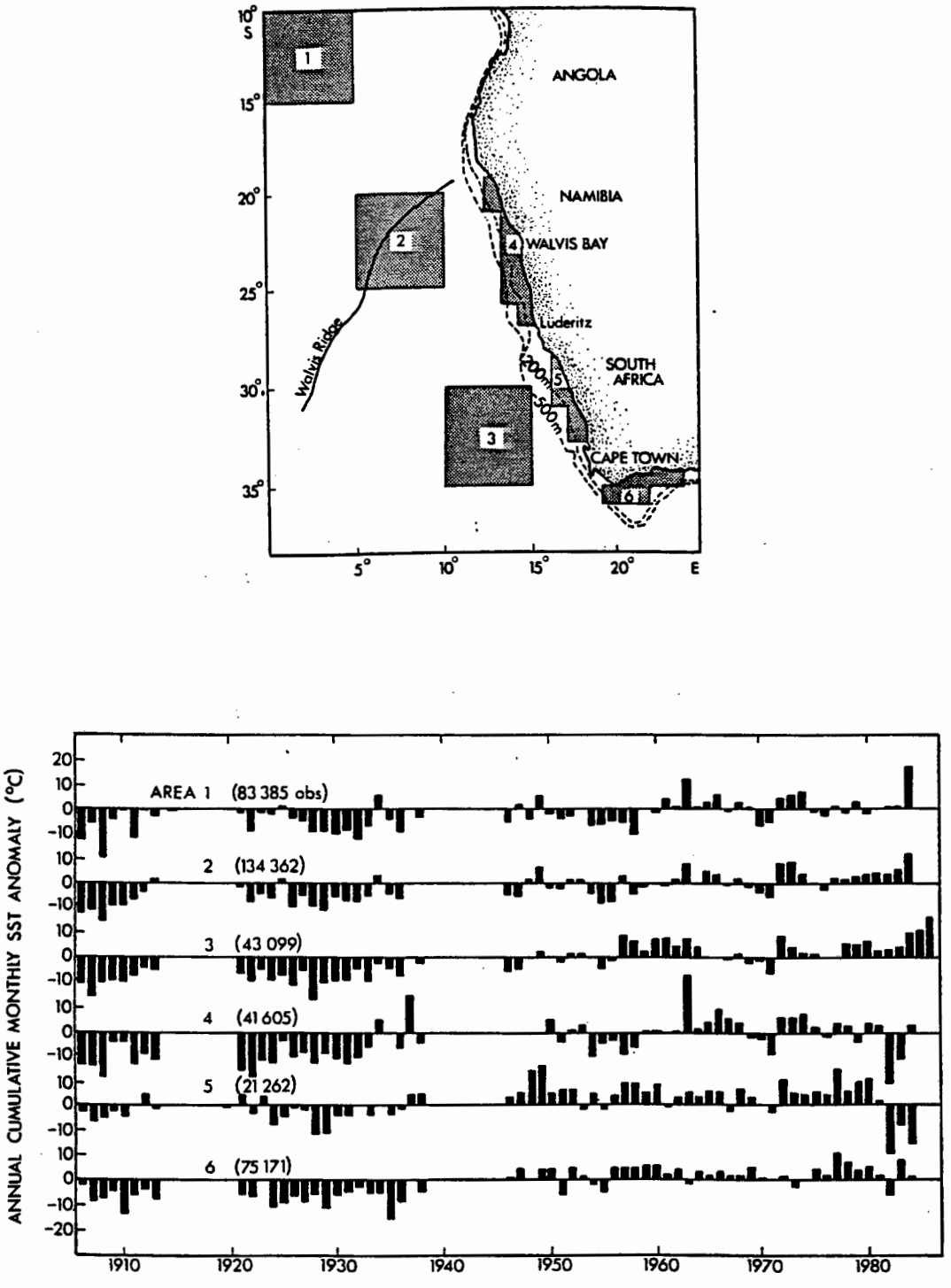

Figure 11. Annual cumulative monthly anomalies of SST for areas one to six around southern Africa (after *Shannon, Lutjeharms and Nelson,* 1990).

The pigment concentrations in the Subtropical Convergence region have been shown to reach values an order of magnitude greater than that of the surrounding Southern Ocean. This region has been recognized as a vertical convergence zone, its

subsurface expression located predominantly north of the surface expression [*Lutjeharms and Valentine*, 1984]. Mixing of the warm, nutrient-poor subtropical waters with the colder subantarctic waters should therefore lead to an increase in density stratification, the resulting enhanced thermal stability causing retention of phytoplankton in the euphotic zone and thus conditions favourable to increased primary production. However, at this latitude, turbulence due to wind stress may be such that phytoplankton are mixed well below the euphotic depth for periods sufficiently long to result in decreased or negative primary production [*Parsons, Takahashi and Hargrave*, 1984]. South of Africa, the position of the Subtropical Convergence is determined primarily by the Agulhas Return Current [*Lutjeharms and Valentine*, 1984]; although a limited seasonal migration of the Subtropical Convergence does occur: Plate 7 shows the mean summer and winter positions of the Subtropical Convergence, or 14°C isotherm, at about 42.5°S and 40·5°S, respectively. In contrast, large seasonal shifts in the zero of the wind stress curl occur annually, the mean summer and winter latitudes being 47°S and 42°S, respectively [*Hellerman and Rosenstein*, 1983]. It is therefore likely that the Subtropical Convergence region south of Africa would experience maximum westerly wind stress during winter, the associated increase in turbulence resulting in minimum pigment concentrations during this season, such as was found in this study (Figure 1c).

Cross-frontal mixing in the Subtropical Convergence region may also take the form of baroclinic eddies, the resulting enhanced thermal stratification at the eddy boundaries leading to increased pigment concentrations [*Lucas et al*, in prep]. It is therefore suggested that increased primary production occurs in the Subtropical Convergence region primarily due to a) a strong thermal gradient and b) a large frontal area, created both by the meandering Rossby wave of the Agulhas Return Current and the eddies spawned at Subtropical Convergence.

The dynamic topography of the ocean south of Africa is characterised by extreme mesoscale variability (Figure 12) [*Feron, de Ruijter and Oskam*, 1992]. The position of the Agulhas retroflection is highly unstable, and during some periods, a substantial component of the Agulhas Current may intrude westwards into the south-east Atlantic Ocean [*Lutjeharms and van Ballegooyen*, 1984]. Model studies have shown that the magnitude of the volume transport of the Agulhas Current is decisive in causing either westward penetration, or early retroflection, the most westerly retroflections occurring for low volume transports of the current *[Lutjeharms and van Ballegooyen*, 1984].

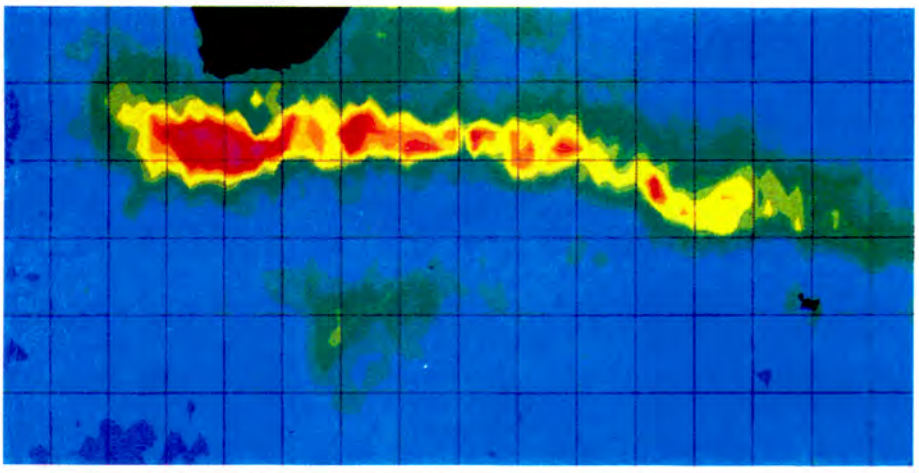

Figure 12. The variability in sea surface topography south of Africa from satellite altimetry (after *Smythe-Wright*, 1991).

De Ruijter [1982] and *de Ruijter and Boudra* [1985] have modelled the Agulhas retroflection in terms of the large-scale wind-driven circulation. They show that leakage of the Agulhas Current into the south-east Atlantic is largely controlled by the meridional position of the zero wind stress curl south of Africa. A southward shift in the zonal wind profile is shown to decrease the isolation of the south Atlantic and south Indian subtropical gyres, resulting in substantial leakage of the

current into the south-east Atlantic. Thus, it may be expected that changing wind strengths over the Indian Ocean would significantly affect the volume fluxes of the Agulhas Current.

Increased volume flux of the Agulhas Current should therefore result in early retroflection, a more southward penetration of the current, and greater intensity of the Agulhas Return Current. This intensity may in turn precipitate the shedding of eddies both at the Agulhas Plateau and further downstream, along the Subtropical Convergence [*Lutjeharms and van Ballegooyen* 1984, *Shannon, Lutjeharms and Nelson*, 1990], while the more southward penetration may result in greater meridional excursions of the Agulhas Return Current. Therefore, if the hypothesis presented above holds true, this should result in both a stronger thermal gradient and a larger frontal area in the Subtropical Convergence region, with resultant enhanced primary productivity.

An unusual westward penetration of very warm Agulhas Current waters into the southeast Atlantic in early 1984 was shown by *Walker* [1986] to follow the occurrence of abnormally high atmospheric pressure and strong easterlies southeast of the continent. Similarly, *Shannon et al.* [1990] found that a major westerly incursion of the Agulhas Current into the southeast Atlantic in 1986 was preceded by abnormally strong easterly trades followed by a sudden reduction in this driving force (Figure 13). *Shannon et al.* [1990] suggested that this was due to a poleward shift in the position of the zero of the wind stress curl, the inferred reduction in volume transport of the Agulhas following the sudden abatement of strong easterly wind forcing in the southwestern Indian Ocean. In contrast, Figure 13 shows a strong positive anomaly in easterly wind forcing in 1980, with a sudden increase in easterly winds in early 1981. If the suggestion by *Shannon et al.* [1990] is correct, this implies that an equatorward shift in the meridional position of the zero of the wind stress curl and an associated increase in Agulhas volume transport would have occurred during 1980-1, with a resultant southward penetration of Agulhas waters.

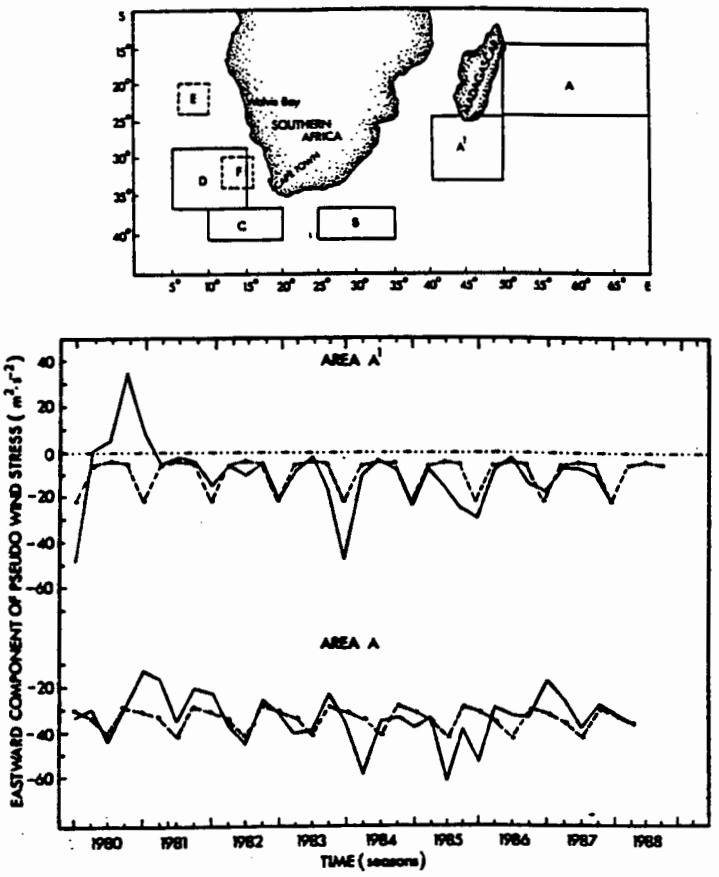

Figure 13. Seasonal (quarterly) values of the eastward component of pseudo wind stress in areas A and A^1 from 1980. The mean seasonal cycles are indicated by dashed lines (after *Shannon et al.*, 1990).

Gillooly and Walker [1984] have in fact shown that during 1980-1, the Subtropical Convergence moved about 2^{o} southwards, along with a more southward penetration of warm Agulhas Current waters (Figure 14). The interannual variation in the Subtropical Convergence region found in this study with enhanced pigment concentrations in 1981 (Figure 3b) may therefore be explained by such circumstances.

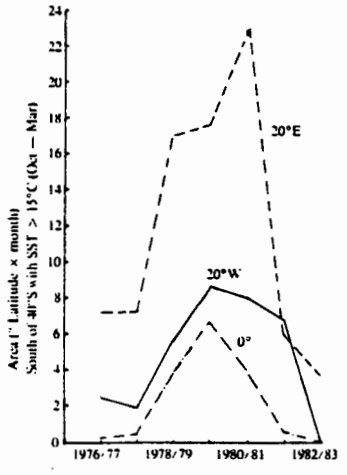

Figure 14. Area south of 40^{o}S for which SST was greater than 15^{o}C between October and March for longitudes 20^{o}W, 0^{o} and 20^{o}E (after *Gillooly and Walker*, 1984).

There appear to be three factors which may dominate the flow of the Agulhas Current a) inertia b) bottom topography c) the windfield. It is proposed that, on leaving the southern tip of the African continent, the strong southward-flowing Agulhas Current is dominated by inertial forces which force it further southwards into the open ocean. Retroflection of the current occurs due to the net accumulation of ß-generated anticyclonic vorticity, resulting in a Rossby wave, the wavelength of which is determined by the expression: $\lambda = 2\pi\,(^{u}/_{\beta})^{1/2}$. The shape and meridional excursions of this Rossby wave are determined by the bottom topography, while downstream, the farfield return current extending into the Indian Ocean is probably dominated by the windfield, or a combination of all three factors discussed above.

CHAPTER 5

CONCLUSIONS

The primary objective of this study was to examine the historical CZCS archive to determine the spatial and temporal variability of phytoplankton pigment in the oceans around and to the south of southern Africa. Although paucity of CZCS data sampling within this area limited detailed analysis, several important results were obtained. These are listed below.

Two distinct chlorophyll signals are seen in the study area: high (5mg m^{-3}) mean pigment concentrations are found in the Benguela Upwelling region confined to the continental shelf, while in the Southern Ocean, the strongest signal (1.5mg m^{-3}) is found in the Subtropical Convergence frontal region. Comparison of the Benguela region with the Subtropical Convergence region shows that, although the mean pigment concentration of the former was around five times that of the latter, the area of the Subtropical Convergence region is at least five times greater than that of the Benguela region. The large expanse of the Subtropical Convergence open ocean front can therefore sustain a standing stock of phytoplankton that is similar in magnitude to the phytoplankton standing stock on the Benguela shelf, the productive Benguela Upwelling system and the Subtropical Convergence front thus forming potentially important carbon dioxide sinks in the Southern Hemisphere.

There are two distinct regimes in the Benguela Upwelling system. The seasonal variation of pigment concentration within the northern Benguela, more pronounced than that in the southern Benguela, shows two peaks in austral spring and fall, the maximum being in the fall. A single maximum in the austral summer is observed in the southern Benguela. These maximum pigment concentrations occur during the respective strongest upwelling periods [*Shannon, Lutjeharms and Nelson,* 1990; *Pearce*, 1991].

Both northern and southern Benguela regions exhibit strong onshore offshore gradients, consistent with strong coastal upwelling patterns. The seasonal variation of the productive area of each is synchronous with the respective pigment variation, the greater mean pigment concentration in the northern Benguela being due to a larger productive area.

The seasonal variations in both the frontal regions are not significant, although a maximum pigment concentration is observed in the Subtropical Convergence region in the fall, with a minimum in winter. This minimum is perhaps due to increased turbulence associated with maximum westerly wind stress during this season.

The relationship between mean seasonal sea surface temperature and mean seasonal chlorophyll concentration appears to take the form of an inverted parabola, the interval about the maximum representing a temperature window within which maximum chlorophyll concentrations are found. The highest mean chlorophyll concentrations in the Benguela Upwelling system are found at a mean sea surface temperature of around $15^{o}C$. Accurate analyses of the sea surface temperature chlorophyll concentration relationship requires both long-term frequently sampled sea surface temperature data together with the corresponding ocean colour data.

Pronounced interannual variations are observed in both the northern and southern Benguela regions, and in the Subtropical Convergence region. This variation is strongest in the northern Benguela, which exhibits a five-fold increase in chlorophyll concentration from 1979 to 1982, peaking in fall 1982. A similar interannual trend is seen in the southern Benguela, where a maximum is reached in summer 1982. These maxima are coincident with the 1982-3 El-Nino Southern Oscillation event. A different interannual trend is shown in the Subtropical Convergence region, where a maximum was observed in fall 1981. This is possibly due to an increase in Agulhas volume flux, with a resultant more southward

penetration of warm Agulhas Current waters and a 2^{o} southward displacement of the Subtropical Convergence front during 1980-1 [*Gillooly and Walker*, 1984].

It is suggested that increased pigment concentrations occur in the Subtropical Convergence region primarily due to a) a strong thermal gradient and b) a large frontal area, created both by the meandering Rossby wave of the Agulhas Return Current and the eddies spawned at Subtropical Convergence. On leaving the southern tip of the African continent, the strong southward-flowing Agulhas Current appears to be dominated by inertial terms forcing it further southwards into the open ocean. The retroflection of the current is thought to occur mainly due to the net accumulation of ß-generated anticyclonic vorticity, resulting in a Rossby wave, the wavelength of which is determined by the expression: $\lambda = 2\pi\ (^{u}/_{\beta})^{1/2}$ (see page 49 for details of symbols). However, the shape and meridional excursions of this Rossby wave in the Subtropical Convergence region appear to be determined by bottom topography, in particular the Agulhas Plateau and the Madagascar Ridge.

It is clear that in order to accurately quantify the spatial and temporal distribution of chlorophyll, and hence oceanic primary production and carbon flux, scientists need frequently sampled synoptic data coverage, coupled with ship and *in situ* investigations. *Morel and Berthon* [1989] have shown that statistically significant relationships exist between the "satellite pigment concentration", the integrated pigment content within the euphotic depth (4.6 times the first attenuation depth) and the shape of the vertical pigment profile. However, in order to transform ocean colour pigment maps into primary production maps, more accurate, geographic specific algorithms are required. *Platt and Sathyendranath* [1988] have suggested that, for a given region and season, both the shape of the vertical profile of pigment biomass and the parameters of the photosynthesis light curve are stable and, that on this basis, the global ocean be partitioned into "dynamic biogeographic provinces". By combining this data base with satellite measurements of ocean colour, maps of

water column primary productivity may be produced and ultimately, the global carbon budget quantified. These have become fundamental aims of the Joint Global Ocean Flux Study (JGOFS) and, together with the 1993 launch of SeaWiFS, should be readily achieved.

LITERATURE CITED

Allanson B.R., R.C. Hart and J.R.E. Lutjeharms, Observations on the Nutrients, Chlorophyll and Primary Productivity of the Southern Ocean south of Africa, *S. Afr. J. Antarct. Res.*, 11, 3-14, 1981.

Austin R.W., *Minutes of the 18th CZCS NET* meeting, NASA GSFC, 35pp, 1982.

Bakun A. and C.S. Nelson, The Seasonal Cycle of Wind-Stress Curl in Subtropical Eastern Boundary Current Regions, *J. Phys. Ocean.*, 21, 1815-1834, 1991.

Brock J.C. and C.R. McClain, Interannual Variability in Phytoplankton Blooms Observed in the Northwestern Arabian Sea During the Southwest Monsoon, *J. of Geophys. Res.*, 97, (C1), 733-750, 1992.

Brown P.C., Spatial and Seasonal Variation in Phytoplankton Biomass in the Southern Benguela / Agulhas Ecosystem, *S. Afr. J. Mar. Sci.*, 12, in press, 1992.

Brown P.C. and K.L. Cochrane, Chlorophyll a Distribution in the Southern Benguela, Possible Consequences of Global Warming on Phytoplankton and its Implications for Pelagic Fish, *S. Afr. J. Sci.*, 87, 233-242, 1991.

Campbell J.W. and J.E. O'Reilly, Role of Satellites in Estimating Primary Productivity on the Northwest Atlantic Continental Shelf, *Cont. Shelf. Res.*, 8, 179-204, 1988.

Clark D.K., Phytoplankton Pigment Algorithms for the Nimbus-7 CZCS, in *Oceanography from Space,* edited by R. Gower, Plenum Press, New York, 227-237, 1981.

Darzi M., J.K. Firestone, G. Fu, E. Yeh and C.R. McClain, Current Efforts Regarding the SEAPAK Oceanographic Analysis Software System, *Proc. 7th Int. Conf. Interactive Process. Sys. Meteorol. Hydrol. Oceanogr.*, 109-115, 1991.

De Ruijter W.P.M., Asymptotic Analysis of the Agulhas and Brazilian Current Systems, *J. Geophys. Res.*, 88, 4343-4354, 1982.

De Ruijter W.P.M. and D.B. Boudra, The Wind-driven Circulation in the South Atlantic-Indian Ocean. Numerical Experiments in a One Layer Model, *Deep-Sea Res.*, 32, 557-574, 1985.

Duncombe Rae C.M., Agulhas Retroflection Rings in the South Atlantic Ocean: An Overview, *S. Afr. J. Mar. Sci.*, 11, 327-344, 1991.

Duncombe Rae C.M., F.A. Shillington, J.J. Agenbag, J. Taunton-Clark and M.L. Gründlingh, An Agulhas Ring in the South Atlantic Ocean and its Interaction with the Benguela Upwelling Frontal System. *Deep-Sea Res.* 38: in press, 1992.

Esaias W.E., G.C. Feldman, C.R. McClain and J.A. Elrod, Monthly Satellite-Derived Phytoplankton Pigment Distribution for the North Atlantic Ocean Basin, *EOS Trans. AGU, 67,* 835, 1986.

Feldman G.C., Variability of the Productive Habitat in the Eastern Equatorial Pacific, *EOS Trans. AGU, 67,* 106, 1986.

Feldman G. et al., Ocean Color: Availability of the Global Data Set, *Eos Trans. AGU,* 70,(23), 634, 1989.

Feron R.C.V., W.P.M. de Ruijter and D. Oskam, Ring Shedding in the Agulhas Current System, *J. Geophys. Res.*, 97, 9467-9477, 1992.

Firestone J.K., G. Fu, M. Darzi and C.R. McClain, NASA's SEAPAK Software for Oceanographic Data Analysis: An Update, *Proc. 6th Int. Conf. Interactive Inf. Process. Sys. Meteorol. Oceanogr. Hydrol.*, 260-267, 1990.

Gill A.E., *Atmosphere-Ocean Dynamics,* Academic Press, New York, 662pp, 1982.

Gill A.E. and R.L. Parker, Contours of "h Cosec Θ" for the World Oceans, *Deep-Sea Res.*, 17, 823-824, 1970.

Gillooly J.F. and N.D. Walker, Spatial and Temporal Behaviour of Sea-surface Temperatures in the South Atlantic, *S. Afr. J. Sci.*, 80, 97-100, 1984.

Gordon H.R. and W.R. McCluney, Estimation of the Depth of Sunglint Penetration in the Sea for Remote Sensing, *Appl. Optics,* 14, 413-416, 1975.

Gordon H.R. and D.K. Clark, Atmospheric Effects in the Remote Sensing of Phytoplankton Pigments, *Boundary-Layer Meteor.*, 18, 300-313, 1980.

Gordon H.R., D.K. Clark, J.L. Mueller and W.A. Hovis, Phytoplankton Pigments Derived from the Nimbus-7 CZCS: Initial Comparisons with Surface Measurements, *Science,* 210, 63-66, 1980.

Gordon H.R. and A.Y. Morel, *Remote Assessment of Ocean Colour for Interpretation of Satellite Visible Imagery*, Springer-Verlag, New York, 1983.

Hellerman S. and M. Rosenstein, Normal Monthly Wind Stress Over the World Ocean with Error Estimates, *J. Phys. Oceanogr.*, 13, 1093-1104, 1983.

Hovis W.A., D.K. Clark, F. Anderson, R.W. Austin, W.H. Wilson, E.T. Baker, D. Ball, H.R. Gordon, J.L. Mueller, S.Z. El-Sayed, B. Sturm, R.C. Wrigley and C.S. Yentsch, Nimbus-7 Coastal Zone Color Scanner: System Description and Initial Imagery, *Science,* 210, 60-63, 1980.

Hovis W.A., The Nimbus-7 Coastal Zone Color Scanner (CZCS) Program, in *Oceanography from Space,* edited by R. Gower, Plenum Press, New York, 213-225, 1981.

Lucas M.I., C. Attwood, K.M. Dower and G. Rigg, Chlorophyll and Primary Production Associated with a Warm Core Ring Shed from the Agulhas Return Current south of Africa: Potential Implications for Carbon Flux, *In prep.*

Lutjeharms J.R.E. and H.R. Valentine, Southern Ocean Thermal Fronts south of Africa, *Deep-Sea Res.*, 31, (12), 1461-1475, 1984.

Lutjeharms J.R.E. and R.C. van Ballegooyen, Topographic Control in the Agulhas Current System, *Deep-Sea Res.*, 31 (11), 1321-1337, 1984.

Lutjeharms J.R.E. and N.M. Walters, Ocean Colour and Thermal Fronts south of Africa. In: *South African Ocean Colour and Upwelling Experiment*, edited L.V. Shannon, SFRI, 270 pp., 1985.

Lutjeharms J.R.E., F.A. Shillington and C.M. Duncombe Rae, Observations of Extreme Upwelling Filaments in the south east Atlantic Ocean. *Science*, N.Y. 253: 774-776, 1991.

McClain C.R., W.E. Esaias, G.C. Feldman, J. Elrod, D. Endres, J. Firestone, M. Darzi, R. Evans and J. Brown, Physical and Biological Processes in the North Atlantic during the First GARP Global Experiment, *J. Geophys. Res.*, 95, C10, 18027-18048, 1990.

McClain C.R., C.J. Koblinsky, J. Firestone, M. Darzi, E. Yeh and B.D. Beckley, Examinimg Several Southern Ocean Data Sets, *EOS Trans. AGU*, 72, (33), 345, 1991.

McClain C.R., G. Fu, M. Darzi, J. Firestone, PC-SEAPAK Users Guide, Version 4.0, *NASA Tech. Memo 104557,* Natl. Space and Aero. Admin., Goddard Space Flight Center, Greenbelt, Md., 1992.

Mitchell-Innes B.A. and D.R. Walker, Short-Term Variability during an Anchor Station Study in the Southern Benguela Upwelling System: Phytoplankton Production and Biomass in Relation to Species Changes, *Prog. Oceangr.*, 28, 65-89, 1991.

Mitchell-Innes B.A. and G.C. Pitcher, Hydrographic Parameters as Indicators of the Suitability of Phytoplankton Populations as Food for Herbivorous Copepods, *S. Afr. J. Mar. Sci.*, 12, in press, 1992.

Morel A., In-Water and Remote Measurements of Ocean Colour, *Boundary-Layer Meteor.*, 18, 177-201, 1980.

Morel A. and J-M. Andre, Pigment Distribution and Primary Production in the Western Mediterranean as Derived and Modelled from Coastal Zone Colour Scanner Observations, *J. Geophys. Res.*, 96, (C7), 12685-12698, 1991.

Morel A. and J.F. Berthon, Surface Pigments, Algal Biomass Profiles, and Potential Production of the Euphotic Zone: Relationships Reinvestigated in View of Remote-Sensing Applications, *Limnol. Oceanogr.*, 34, 1545-1562, 1989.

Muller-Karger F.E., J.J. Walsh, R.H. Evans and M.B. Meyers, On the Seasonal Phytoplankton Concentration and Sea Surface Temperature Cycles of the Gulf of Mexico as Determined by Satellites, *J. Geophys. Res.*, 96, (C7), 12645-12665, 1991.

Panofsky H.A. and G.W. Brier, *Some Applications of Statistics in Meteorology,* Pennsylvania State University, Pennsylvania, 224pp., 1968.

Parsons T.R., M. Takahashi and B. Hargrave, *Biological Oceanographic Processes,* Oxford Pergamon Press, 330pp., 1984.

Pearce A.F., Eastern Boundary Currents of the Southern Hemisphere, *J. Roy. Soc. WA.*, 74, 35-45, 1991.

Pedlosky J., *Geophysical Fluid Dynamics*, Springer-Verlag, New York, 624pp., 1987.

Peterson W.T., L. Hutchings, J. Huggett and J. Largier, Anchovy Spawning in Relation to the Biomass and the Replenishment Rate of their Copepod Prey on the western Agulhas Bank. In: *Benguela Trophic Functioning,* Payne, A.I.L., Brink, K.H., Mann, K.H. and R. Hilborn (Eds). S. Afr. J. mar. Sci., 12, in press, 1992.

Planke J., Phytoplankton Biomass and Productivity in the Subtropical Convergence Area and Shelves of the Western Indian Subantarctic Islands. In: *Adaptations within Antarctic Ecosystems,* edited by Llano, G.A., Smithsonian Institution, Washington D.C., 51-77, 1977.

Platt T. and S. Sathyendranath, Oceanic Primary Production: Estimation by Remote Sensing at Local and Regional Scales, *Science,* 241, 1613-1620, 1988.

Shannon L.V., P. Schlittenhardt and S.A. Mostert, The Nimbus-7 CZCS Experiment in the Benguela Current Region off Southern Africa, February 1980. Interpretation of Imagery and Oceanographic Implications, *J. Geophys. Res.*, 89, (D4), 4968-4976, 1984.

Shannon L.V.(Ed.), *South African Ocean Colour and Upwelling Experiment,* Sea Fisheries Research Institute, Cape Town, 270pp., 1985a.

Shannon L.V., The Benguela Ecosystem Part I. Evolution of the Benguela, Physical Features and Processes, *Oceanogr. Mar. Biol. Ann. Rev.*, 23, 105-182, 1985b.

Shannon L.V., N.M. Walters and S.A. Mostert, Satellite Observations of Surface Temperature and Near-Surface Chlorophyll in the Southern Benguela Region, In: *South African Ocean Colour and Upwelling Experiment,* edited by L.V. Shannon, Sea Fisheries Research Institute, Cape Town, 183-210, 1985.

Shannon L.V. and S.C. Pillar, The Benguela Ecosystem Part III. Plankton, *Oceanogr. Mar. Biol. Ann. Rev.*, 24, 65-170, 1986.

Shannon L.V., A.J. Boyd, G.B. Brundrit and J. Taunton-Clark, On the Existence of an El-Nino Phenomenon in the Benguela System, *J. Mar. Res.*, 44, 495-520, 1986.

Shannon L.V., J.R.E. Lutjeharms and G. Nelson, Causative Mechanisms for Intra-Annual and Interannual Variability in the Marine Environment around Southern Africa, *S. Afr. J. Sci.*, 86, 356-373, 1990.

Shannon L.V., J.J. Agenbag, N.D. Walker and J.R.E. Lutjeharms, A Major Perturbation in the Agulhas Retroflection Area in 1986, *Deep-Sea Res.*, 37, (3), 493-512, 1990.

Smith E., A User's Guide to the NOAA Advanced Very High Resolution Radiometer Multichannel Sea Surface Temperature Data Set, produced by: *The University of Miami/Rosentiel School of Marine and Atmospheric Science*, distributed by the PO.DAAC, JPL, California Institute of Technology, California, 1992.

Smythe-Wright D. (Ed.), *Ocean Circulation and Climate,* The Natural Environment Research Council, Southampton, U.K., 24pp, 1991.

Sousa F.M. and A. Bricaud, Satellite-Derived Phytoplankton Pigment Structures in the Portuguese Upwelling Area, *J. Goephys. Res.*, 97, (C7), 11343-11356, 1992.

Sverdrup H.U., M.W. Johnson and R.H. Fleming, *The Oceans: their Physics, Chemistry and General Biology,* Prentice-Hall, New Jersey, 1087pp., 1942.

Taunton-Clark J., Environmental Events within the South-East Atlantic (1906 - 1985) Identified by Analysis of Sea Surface Temperature and Wind Data, *S. Afr. J. Sci.*, 86, 470-472, 1990.

Walker N.D., Satellite Observations of the Agulhas Current and Episodic Upwelling south of Africa, *Deep-Sea Res.*, 33 (8), 1083-1106, 1986.

Walters N.M., Verification of the Utility of the Coastal Zone Colour Scanner in Portraying Pigment Concentrations along the Cape West Coast, *S. Afr. J. Phys.*, 6, (2), 63-66, 1983.

Walters N.M., Algorithms for the Determination of Near-Surface Chlorophyll and Semi-Quantitative Total Suspended Solids in South African Coastal Waters from Nimbus-7 CZCS Data, In: *South African Ocean Colour and Upwelling Experiment*, edited L.V. Shannon, SFRI, 175-182, 1985.

Walters N.M. and E.H. Schumann, Detection of Silt in Coastal Waters by NIMBUS-7 CZCS, In: *South African Ocean Colour and Upwelling Experiment*, edited L.V. Shannon, SFRI, 219-225, 1985.

Walters N.M., C.J. Kok and C. Claase, Optical Properties of the South African Marine Environment In: *South African Ocean Colour and Upwelling Experiment*, edited L.V. Shannon, SFRI, 157-170, 1985.

Williams S.P., E.F. Szajna and W.A. Hovis, Nimbus 7 Coastal Zone Colour Scanner. Level 1 Data Product Users' Guide, *NASA Technical Memorandum 86203*, NASA, 49pp, 1985.